



**HAL**  
open science

## Genetic determinism of prickles in rose

N. Zhou, K. X. Tang, J. Jeauffre, T. Thouroude, D Lopez Arias, F. Foucher,  
L. Hibrand-Saint Oyant

► **To cite this version:**

N. Zhou, K. X. Tang, J. Jeauffre, T. Thouroude, D Lopez Arias, et al.. Genetic determinism of prickles in rose. TAG Theoretical and Applied Genetics, 2020, early access, 19 p. 10.1007/s00122-020-03652-7. hal-02933278

**HAL Id: hal-02933278**

**<https://univ-angers.hal.science/hal-02933278>**

Submitted on 8 Sep 2020

**HAL** is a multi-disciplinary open access archive for the deposit and dissemination of scientific research documents, whether they are published or not. The documents may come from teaching and research institutions in France or abroad, or from public or private research centers.

L'archive ouverte pluridisciplinaire **HAL**, est destinée au dépôt et à la diffusion de documents scientifiques de niveau recherche, publiés ou non, émanant des établissements d'enseignement et de recherche français ou étrangers, des laboratoires publics ou privés.

# Genetic determinism of prickles in rose

NN Zhou<sup>1,2</sup>, KX Tang<sup>2</sup>, J. Jeuffre<sup>1</sup>, T. Thouroude<sup>1</sup>, D. Lopez Arias<sup>1</sup>, F. Foucher<sup>1\*</sup> & L. Hibrand-Saint Oyant<sup>1\*</sup>.

*1 Université d'Angers, Agrocampus-Ouest, INRAE, GDO-IRHS (Genetics and Diversity of Ornamental Plants, Institut de Recherche en Horticulture et Semences), SFR 4207 QUASAV, 49071 Angers, France*

*2 National Engineering Research Center for Ornamental Horticulture; Flower Research Institute, Yunnan Academy of Agricultural Sciences, Kunming 650231, China*

*\* both authors contributed equally to the work.*

Corresponding author: [zhouning1116@aliyun.com](mailto:zhouning1116@aliyun.com)

**Key message: The genetic determinism of prickle in rose is complex, with a major locus on LG3 that controls the absence/presence of prickles on the rose stem.**

## Declarations

### Author Contributions

#### Contributions

NN Zhou designed the projects and obtained funding, planned and performed experiments, collected and analyzed data, and drafted the manuscript. F. Foucher and L. Hibrand-Saint Oyant were responsible for piloting and supervising the project, and for revising the manuscript. KX Tang contributed to designing the project and obtaining funding. J. Jeuffre led the qPCR experiment and analyzed data. T. Thouroude prepared the plant cuttings of F<sub>1</sub> individuals in the greenhouse. D. Lopez Arias modified the genetic map and helped to develop the R/qtl script.

#### Orcid-ID

Zhou NN: [orcid.org/0000-0002-5208-6788](https://orcid.org/0000-0002-5208-6788)

Tang KX: [orcid.org/0000-0003-3807-784X](https://orcid.org/0000-0003-3807-784X)

Jeuffre J: [orcid.org/0000-0001-6770-0552](https://orcid.org/0000-0001-6770-0552)

Thouroude T: [orcid.org/0000-0001-7908-7353](https://orcid.org/0000-0001-7908-7353)

Lopez Arias D: [orcid.org/0000-0001-8129-2786](https://orcid.org/0000-0001-8129-2786)

29 Foucher F: [orcid.org/0000-0002-3693-7183](https://orcid.org/0000-0002-3693-7183)

30 Hibrand-Saint Oyant L: [orcid.org/0000-0002-4451-8798](https://orcid.org/0000-0002-4451-8798)

## 31 **Abstract**

32 Rose is one of the major ornamental plants. The selection of glabrous cultivars is an  
33 important breeding target but remains a difficult task due to our limited genetic  
34 knowledge. Our objective was to understand the genetic and molecular determinism of  
35 prickles. Using a segregating diploid rose F<sub>1</sub> population, we detected two types of  
36 prickles (glandular and non-glandular) in the progeny. We scored the number of non-  
37 glandular prickles on the floral and main stems for three years. We performed QTL  
38 analysis and detected four prickle loci on LG1, 3, 4 and 6. We determined the credible  
39 interval on the reference genome. The QTL on LG3 is a major locus that controls the  
40 presence of prickles, and three QTLs (LG3, 4 and 1) may be responsible for prickle  
41 density. We further revealed that glabrous hybrids are caused by the combination of the  
42 two recessive alleles from both parents. In order to test if rose prickles could originate  
43 from a 'trichome-like structure', we used a candidate approach to characterize rose gene  
44 homologues known in Arabidopsis, involved in trichome initiation. Four of these  
45 homologues were located within the overlapping credible interval of the detected QTLs.  
46 Transcript accumulation analysis weakly supports the involvement of trichome  
47 homologous genes, in the molecular control of prickle initiation. Our studies provide  
48 strong evidence for a complex genetic determinism of stem prickle and could help to  
49 establish guidelines for glabrous rose breeding. New insights into the relationship  
50 between prickles and trichomes constitute valuable information for reverse genetic

51 research on prickles.

## 52 **Keywords**

53 Trichome, QTL, *ZFP5*, *GIS2*, *MYB61*, *MYC1*

## 54 **Introduction**

55 Rose is the major ornamental plant worldwide with a wide diversity, diverse application  
56 forms and an extensive cultivated area. Roses are sold as cut flowers, garden plants, in  
57 pots, for essential oil, flower tea and culinary purposes. In past centuries, with the  
58 continuous efforts of breeders, more than 33,000 varieties of roses were created (Young  
59 2007). However, most of these varieties have persistent prickles on the stem. Prickles  
60 can protect against herbivores by deterring them from eating the stem (Ronel and Lev-  
61 Yadun 2012; Burns 2014). Furthermore, prickles can be desirable in roses when they  
62 are used in hedges to protect properties (as was the case in Reunion Island during the  
63 19<sup>th</sup> century). However, garden roses without prickles are often desirable. Cut roses  
64 with prickles are more difficult to handle, harvest and transport and also constitute  
65 safety hazards for consumers and workers. Retailers commonly remove prickles from  
66 stems prior to sale. Removing the prickles increases labor costs and causes mechanical  
67 damage to the stems, which affects vase life and ornamental value. Although a strong  
68 market demand to develop roses without prickles exists (Nobbs 1984; Debener 1999;  
69 Canli 2003; Canli and Skirvin 2003; Canli and Kazaz 2009), relatively little is known  
70 about the genetic and molecular bases of prickle initiation and development.

71 In plants, prickles are described as outgrowths of the epidermis and subjacent layers

72 that lack vasculature, and mainly consist of lignin, suberin, cellulose and hemicellulose  
73 (Asano et al. 2008; Li et al. 2012). In rose and raspberry, it was thought that prickles  
74 were modified glandular trichomes that differentiate at the time of lignification into  
75 their final prickle morphologies (Kellogg et al. 2011).

76 Until recently, only a few studies had been published about the molecular regulation of  
77 prickle development, but great progress has been made in trichome initiation and  
78 development, especially in *Arabidopsis*. Several transcription factors (TFs) such as  
79 MYB, bHLH, WD40, WRKY and C2H2 zinc finger families' proteins have been  
80 identified as being involved in trichome initiation and development (reviewed in  
81 Balkunde et al. (2010), Pattanaik et al. (2014), Ma et al. (2016a), Huchelmann et al.  
82 (2017) and Chopra et al. (2019)). A trimeric activator complex consisting of MYB  
83 (GLABRA1) - bHLH (GLABROUS3/ENHANCER OF GL3) - WDR  
84 (TRANSPARENT TESTA GL1) plays a key role in trichome development (Zhang 2003;  
85 Kirik et al. 2005; Patra et al. 2013). This trimeric complex finely regulates the temporal  
86 and spatial expression of *GLABRA2* (*GL2*) and *TRANSPARENT TESTA GL2* (*TTG2*),  
87 determining the fate and pattern of trichome precursor cells (Rerie et al. 1994; Ishida et  
88 al. 2008). The bHLH family genes, *MYC1* and *TT8*, belong to the same clade as *GL3*.  
89 *AtMYC1* acts as a positive regulator of trichome initiation (Symonds et al. 2011; Zhao  
90 et al. 2012), and *AtTT8* controls trichome development on leaf margins (Maes et al.  
91 2008). AaMYB1 and its orthologue AtMYB61, belonging to the R2R3MYB subfamily,  
92 were thought to affect terpene metabolism and trichome development in *A. annua* and  
93 *A. thaliana*, respectively (Matías-Hernández et al. 2017).

94 The active TTG1 trimeric complex can be repressed by R3 MYB subfamily genes:  
95 *TRY/CPC/TCL1* act as negative regulars by competing with *GL1* for binding to *GL3*  
96 (Wang et al. 2008; Wester et al. 2009; Wang and Chen 2014). The active TTG1  
97 complex, in interaction with *TTG2*, regulates the expression of the R3 MYB inhibitors  
98 that move to the neighboring cells where they repress trichome initiation (Pesch and  
99 Hülkamp 2004; Pesch et al. 2014).

100 Different growth regulators positively affect trichome initiation, such as GA3, cytokinin  
101 and jasmonic acid (Traw and Bergelson 2003), through the activation of *GL1* (Gan et  
102 al. 2006). Different C2H2 zinc-finger proteins such as *GLABROUS*  
103 *INFLORESCENCE STEM (GIS)*, *GIS2*, *GIS3*, *ZINC FINGER PROTEIN5*, 6 and 8  
104 (Gan et al. 2006; Gan et al. 2007) include GA and cytokinin signaling pathways (Zhou  
105 et al. 2013). The novel transcription factor *TRP* interacts with *ZFP5* and negatively  
106 regulates trichome initiation through the gibberellic acid pathway (Kim et al. 2018).

107 In diploid rose, the presence of prickles on the stem was assumed to be controlled by a  
108 single dominant gene (Debener 1999; Shupert et al. 2007) located on linkage group 3,  
109 LG3 (Linde et al. 2006). Furthermore, two QTLs were detected on LG3 with the scoring  
110 of prickle density (Crespel et al. 2002). Using two F<sub>1</sub> progenies, Hibrand-Saint Oyant  
111 et al. (2018) also identified a large QTL (or two neighboring QTLs) on LG3 (between  
112 position 31 Mb - 46.5 MB corresponding to the end of the chromosome 3) and a  
113 significant association between position 31 and 32.4 Mb using a GWAS approach. In  
114 tetraploid roses, three QTLs were identified in relation to the number of prickles on the  
115 stem: two located on LG2 and one on LG3 (Koning-Boucoiran et al. 2009). Using the

116 same K5 population with the same phenotype data but a new genetic map, different  
117 QTLs were detected on LG3, 4 and 6 and on LG2 (one year) (Bourke et al. 2018).  
118 Recently, a WRKY transcription factor, homologous to Arabidopsis *TTG2*, was located  
119 close to a QTL controlling prickles density, and the gene transcripts are differentially  
120 accumulated between prickles and prickless roses (Hibrand-Saint Oyant et al. 2018).  
121 In this study, our objectives were to decipher the genetic determinism of stem prickles  
122 in rose and to characterize candidate genes involved in prickles initiation and  
123 development. First, we defined the different types of prickles on the stem and studied  
124 them separately. Using an F<sub>1</sub> progeny, we detected QTLs and their position in the rose  
125 genome sequence. We further analyzed how the alleles of the major QTLs affect the  
126 presence of prickles. We identified putative candidate genes (homologues of genes  
127 involved in trichome initiation and development in Arabidopsis) and studied their  
128 transcript accumulation. That study suggested that prickles and trichomes may carry  
129 two different genetic pathways, providing new insights into the relationship between  
130 prickles and trichomes.

## 131 **Materials and methods**

### 132 **Plant material**

133 A progeny of 151 diploid F<sub>1</sub> hybrids obtained from a cross between the female *Rosa*  
134 *chinensis* ‘Old Blush’ (OB) × the male *R. x wichurana* (RW) was used for map  
135 construction (described in Hibrand-Saint Oyant et al. 2018) and QTL analysis. The  
136 plants were grown in a field and managed by the Horticulture Experimental Unit  
137 (INRAE, Angers, France). The plants were pruned each December. In the following

138 spring, new stems developed from the axillary buds from the old pruned stems, and are  
139 referred to as “floral stems” since they develop flowers. Later, new stems arise from the  
140 base of the plant and are referred to as “main stems”. They remain vegetative in once-  
141 flowering individuals and may become floral in continuous-flowering individuals.

## 142 **Phenotypic data collection and analyses**

143 To score prickly density, we selected three independent floral and main stems for each  
144 F<sub>1</sub> progeny and the two parents. The prickly numbers were counted for each selected  
145 stem on four internodes (located in the middle of the stem) for three years (2016, 2017  
146 and 2018).

147 Statistical analysis and visualization were performed using R version 3.2.3. We  
148 visualized the frequency distribution and Q-Q plot using the *'hist'*, *'legend'*, *'qqnorm'*  
149 and *'qqline'* functions. We performed mixed-factorial ANOVA analysis with *'aov'*. A  
150 *'shapiro.test'* was used to test the normality of the original data and the ANOVA  
151 residuals. When the null hypothesis was negated, *'kruskal.test'* was used to test if there  
152 was any significant difference between the replicate shoots, years and the type of stem  
153 variance. *'pairwise.wilcox.test'* with *'p.adjust.method =BH'* was used to calculate  
154 pairwise comparisons between group levels with corrections for multiple testing. We  
155 displayed the distribution of prickly density with a boxplot to compare the difference  
156 between the variance using the *ggplot2* and *ggpubr* packages.

157 Variance components were estimated with the restricted maximum likelihood (REML)  
158 method using the ‘*sommer*’ package. Phenotype variance components of prickles density  
159 were obtained using the following model:

$$160 \quad P_{ijlr} = \mu + G_i + S_l + Y_{(l)j} + GS_{il} + GY_{ij} + \varepsilon_{ijlr},$$

161 where  $P_{ijlr}$  is the phenotypic value of a trait counted on a triplicate stem  $r$  of the stem  
162 type  $l$  of the individual  $i$  in the year  $j$ ,  $\mu$  is the overall mean,  $G_i$  is the random effect of  
163 genotype  $i$ ,  $S_l$  is the random effect of stem type  $l$ ,  $Y_{(l)j}$  is the random effect of year  $j$   
164 nested in stem type  $l$ ,  $GS_{il}$  is the random interaction between genotype  $i$  and stem type  
165  $l$ ,  $GY_{ij}$  is the random interaction between genotype  $i$  and year  $j$ , and  $\varepsilon_{ijlr}$  is the random  
166 residual error.

167 The phenotypic variance ( $\sigma_P^2$ ) of stem prickles was divided into the variance of  
168 genotypic effect ( $\sigma_G^2$ ), genotype  $\times$  year interaction ( $\sigma_{GY}^2$ ), genotype  $\times$  stem type  
169 interaction ( $\sigma_{GS}^2$ ), and the residual error variance ( $\sigma_E^2$ ).

170 Narrow-sense heritability ( $h^2$ ) was calculated as follows:

$$171 \quad h^2 = \sigma_G^2 / (\sigma_G^2 + \sigma_{GY}^2 / y + \sigma_{GS}^2 / s + \sigma_E^2 / ysr)$$

172 where  $y$  is the number of years,  $r$  is the number of replication shoots per individual, and  
173  $s$  is the number of stem types (PF and PM).

## 174 **Genotypic data**

175 The genetic determinism was conducted using the genetic map previously obtained by  
176 Hibrand-Saint Oyant et al. (2018) and modified by Lopez-Arias et al. (in prep).

## 177 **QTL Analysis**

178 In this study, we performed QTL detection for prickles on the floral (PF) and main (PM)

179 stems from data scored in 2016, 2017, 2018 (referred to as PF2016, PF2017, PF2018,  
180 PM2016, PM2017 and PM2018, respectively). QTL analyses were carried out using the  
181 R/qtl in R version 3.2.3. Based on the non-normal phenotype distribution data, single  
182 QTL analysis and LOD scores were calculated using the 'scanone' function with non-  
183 parametric model (*model="np", ties.random = FALSE, method = "em"*) and the two-  
184 part model (*model="2part", upper = FALSE*) (Boyartchuk et al. 2001).

185 In the non-parametric model, the genome-wide and chromosome-wide significance  
186 thresholds of LOD scores were estimated by permutations tests (*n.perm = 1000,*  
187 *n.cluster = 20*). The Bayesian credible interval was computed with 0.95 and 0.99  
188 coverage probabilities. When QTLs for different traits had overlapping 0.95 credible  
189 intervals, they were declared to be a potentially "common QTL (cQTL)" (Kawamura  
190 et al. 2011). The percent of variance explained by each QTL was calculated by 'makeqtl'  
191 and 'fitqtl' with a 'normal' model.

192 In the two-part model, the phenotype was separated into two parts: first, the trait value  
193 was considered as without (0) or with (1) prickles; if it had prickles, the trait value  
194 above zero was assumed to be normally distributed. Three LOD scores for each  
195 genomic position were calculated:  $LOD(p)$  and  $LOD(\mu)$  were calculated for binary  
196 traits (0 or 1) and non-zero phenotype quantitative traits ( $> 0$ ), respectively;  $LOD(p,\mu)$   
197 is simply the sum of the LOD scores from the two separate analyses (Broman 2003).

198 The genome-wide significance thresholds of three LOD hypotheses were also estimated  
199 by 1000 permutation tests and summarized by a 0.05 alpha threshold. The percent of  
200 variance explained was calculated by 'makeqtl' and 'fitqtl' with 'binary' and 'normal'

201 models for binary( $p$ ) and quantitative( $\mu$ ) traits.

## 202 **Selection of rose candidate genes involved in prickly density**

203 Proteins involved in trichome initiation and development were selected in *A. thaliana*  
204 from the TAIR database (<https://www.arabidopsis.org>) with searching terms GL1,  
205 MYB82, MYB61, CPC, TRY, GL3, TT8, MYC1, TTG1, TTG2, ZFP5, ZFP1, GIS2,  
206 GIS3, GL2. Rose homologues were searched using BLASTp in the *Rosa chinensis*  
207 Genome v1.0 (Hibrand-Saint Oyant et al. 2018). In addition, we also searched the  
208 transcription factors (TF) belonging to the bHLH, WD40, R2R3MYB, C2H2 and  
209 WRKY families in rose and which were located on the major cQTL interval of LG3.  
210 Using Geneious 9.1.7, ‘Multiple Align’ was performed for the family gene sequences.  
211 Conserved domains were used to build phylogenetic trees using the ‘Geneious Tree  
212 Builder’ tool with the Jukes-Cantor genetic distance model and the UPGMA tree build  
213 method. The rose candidate genes were named according to the following nomenclature  
214 corresponding to *Rc* (for *Rosa chinensis*) added to the corresponding gene name in  
215 Arabidopsis, e.g., *RcTTG2* for the rose *TTG2* homologue.

## 216 **Gene expression analysis**

217 Primers were designed using Primer Premier 5.0 software. To ensure the specificity of  
218 the primers, forward and reverse primers were designed in the last exon and in the  
219 beginning (first 100 bp) of the 3'UTR. Primer length was between 18 and 25 bp, product  
220 length was between 70 and 200 bp, GC content was between 40% and 60%, and the  
221 annealing temperature was 58~65 °C. Primers are listed in Supplementary Table 1.

222 For the qPCR experimental design, we selected four contrasting once-flowering

223 individuals from the OW progeny for prickles density: two with no prickles (OW9067  
224 and OW9068) and two with prickles (OW9137 and OW9071 with means of 2.5 and 4  
225 prickles per internode on the main stem, respectively). The materials were sampled in  
226 April 2018 in a greenhouse (three biological replicates). Stems were harvested at  
227 different stages of prickles development for roses with prickles, and stems at the same  
228 stages for roses without prickles (Supplementary Figure 1). Total RNA was extracted  
229 using the NucleoSpin RNA Plus-XS kit for early stages (I and IIa) and using the  
230 NucleoSpin RNA Plus-kit for later stages (IIb, IIc and III) according to the  
231 manufacturer's instructions, with minus modifications (2%PVP40 in lysis buffer). The  
232 purity of the RNA was checked on 1% agarose gel, and the concentration was measured  
233 by an UV spectrophotometer. cDNA was obtained from 500 ng of total RNA using  
234 iScript™ Reverse Transcription Supermix for RT-qPCR (Bio-Rad, Hercules)  
235 according to the manufacturer's instructions. The purity and quality of the cDNA were  
236 checked by performing PCR amplification with a blank and RW's DNA sample control,  
237 and the concentration was measured with a UV spectrophotometer. RT-qPCR reactions  
238 were performed using the soAdvanced™ Universal SYBR® Green Supermix (Bio-  
239 Rad) on the CFX Connect Real-time PCR system (Bio-Rad). The gene efficiency was  
240 evaluated with a serial dilution of the thirty cDNAs pooling (1:10, 25, 50, 100, 250,  
241 500, 1000). A 1:25 dilution of each cDNA was used to analyse the expression pattern  
242 of ten candidate genes and two reference genes *UBC* and *TCTP* (Randoux et al. 2012).  
243 Data collection was performed using the Bio-Rad CFX Maestro1.1. Amplification  
244 efficiency of the ten genes ranged from 90.5-104.1%. The reference genes *UBC* and

245 *TCTP* presented high expression stability in all the samples.

246 For the technical replicates, potential outliers were excluded from the analysis when the  
247 standard deviation (SD) of samples is higher than 0.5. Only seven technical replicates  
248 (seven out of 390) were excluded: CPC in PIIb (biological group A, C) and in NPIIc  
249 (group A), GIS2 in NPIIc (group C), NPIII (group B) and PIII (group B).

250 Normalized expression ( $\Delta\Delta Cq$ ) was calculated using Bio-Rad Maestro1.1 software by  
251 applying the '*gene study*' tool. The cluster analysis for sample and target genes with the  
252 mean value of normalized expression was performed using R software with the  
253 '*heatmap*' package. NP samples were used as controls to compare the normalized  
254 expression of genes between P and NP samples in the different stages. |Fold change  
255 (FC)| >2 and the Wilcoxon signed rank test (p-value < 0.05) as cut-off values in scatter  
256 plots were used to demonstrate the significant difference of normalized expression  
257 between P and NP samples. NPI was used as a control to visualize the relative  
258 normalized expression during stem development in prickly and glabrous stems.

## 259 **Results**

### 260 **1-Type, distribution and genetic variability of stem prickles in OW progeny**

261 Both parents of the F<sub>1</sub> progeny ('Old Blush' and *R. x wichurana*) present prickles on  
262 their stems (Figure 1a) (a mean of around ten prickles on four internodes). In the F<sub>1</sub>  
263 progeny, hybrids without prickles can be observed (14 out of 151; no prickles on the  
264 three stems scored over three years). These hybrids with glabrous stems (Figure 1b)  
265 are referred to as 'prickless' individuals (Figure 1c). Out of the 137 F<sub>1</sub> individuals with  
266 prickles (Figure 1b), nine hybrids were nearly prickless (prickle number on four

267 internodes < 1 for three scored years and two types of stems; Figure 1d, Supplementary  
268 Figure 2), and numerous stems were glabrous for some individuals, whereas other stems  
269 presented a few prickles (variable between the genotypes with unstable states between  
270 years and types of stems). Macroscopic analysis shows that parents that present prickles  
271 originated from a ‘non-glandular’ structure. These prickles are referred to as Non-  
272 Glandular Prickles (NGP). All the F<sub>1</sub> prickly individuals (137 out of 151) have NGP.  
273 However, some individuals with NGP prickles also present another type of prickle (27  
274 out of 137). These prickles present a ‘glandular head’ structure and are referred to as  
275 Glandular Prickles (GP) (Figure 1b and 1c, Supplementary Figure 2). Since the  
276 presence of GP in the OW progeny is rare (27 and 12 out of 151 on flowers and main  
277 stems, respectively; Figure 1d) and very irregular, we decided to consider only NGPs  
278 in this study.

279 For the 151 F<sub>1</sub> progenies, the number of NGPs on four internodes of floral (PF) and  
280 main (PM) stems ranged from 0 to 52 and from 0 to 48, respectively (Supplementary  
281 Figure 2). Among them, OW9106 and OW9107 have a much higher prickle density (28  
282 to 52 in the scored years) than the others. As for the two parents, OB and RW have an  
283 average of 11.1 and 8.7 on PF, and an average of 11.8 and 9.2 on PM, respectively  
284 (Figure 1a, Table 1). The ranges of NGP numbers in the F<sub>1</sub> hybrids were obviously  
285 beyond the values of the two parents, indicating a transgressive segregation.

286 The Shapiro-Wilk normality test and the Q-Q plot of original data ( $W = (0.692\sim 0.936)$ ,  
287  $p < 2.96 \times 10^{-8}$ ) (Supplementary Figure 2) and variance residuals ( $W = 0.88591$ ,  $p$ -  
288 value <  $2.2e^{-16}$ ) showed that the NGP densities on stems in the F<sub>1</sub> population were not

289 normally distributed. We tried to transform data (log10, SQRT, box-cox) to make them  
290 normal but without success. The Kruskal-Wallis test reveals a genotype effect, a year  
291 effect and a stem effect (Table 1). The high heritability ( $h^2 \approx 0.97$ ) demonstrated that  
292 the genetic analyses of stem prickles of this population were reliable (Table 1).

## 293 **2- QTL analysis**

### 294 *2.1 Non-parametric QTL analysis*

295 For the female and male maps, strong QTLs were detected on LG3 for the two types of  
296 stems and for the three years ([Figure 2](#) and [Table 2](#)). The LOD scores are higher for the  
297 male map (between 8 and 11.5) and relatively lower for the female map (between 2.3  
298 and 6.2). These QTLs explained between 6.65 to 37.4% of the phenotypic variance. The  
299 locations of these QTLs are very close. Indeed, on the female map, the marker at the  
300 peak of the QTLs is the same for both types of stems (Rh12GR\_16570\_782, 51.1 cM,  
301 located on the chr3 at 44,459,262 bp according to the *Rosa chinensis* Genome v1.0  
302 (Hibrand-Saint Oyant et al. 2018)), except for PM2018 (Rh12GR\_34665\_95, 45.7 cM,  
303 located on chr3 at 41,401,120 bp). On the male map, for the two types of stems and for  
304 the three years, the marker with the highest LOD for the QTLs detected on LG3 is the  
305 same, Rh12GR\_52506\_1218 (42.6 cM on the LG3, 42,317,122 bp on Chr3), which is  
306 the terminal marker on the genetic map but not on the physical map.

307 Furthermore, if we consider the common 0.95 Bayesian credible interval of these QTLs  
308 on LG3 on the female and male maps, all intervals are overlapping (Table 2 and Figure  
309 4). For the female map, the interval on LG3 was 40.38-53.75 cM, which corresponds  
310 to the interval 36,517,224-46,440,369 bp on the physical map of chr3 (Figure 4a), and

311 for the male map, the interval on LG3 was 37.69-42.55 cM, corresponding to the  
312 interval 41,648,024-42,317,122 bp on the physical map (Table 2, Figure 4b).

313 On LG4, QTLs were only detected on the female map for the main stem for the three  
314 years (Figure 2, Table 2). The peak marker Rh12GR\_60129\_183 located at 30.6 cM,  
315 which is located on chr4 at 52,239,028 bp, explained 10.35 to 13.18% of the observed  
316 variance depending on the year of the phenotypic variance in the single QTL model.  
317 The common 0.95 credible interval on LG4 was 20.53-48.59 cM, which covered from  
318 46,189,407-56,107,784 bp on the physical map (Figure 4a, Table 2).

319 On LG6, QTLs were only detected on the male map for three years for PM and for two  
320 years (2017 and 2018) for PF (Figure 2 and Table 2). For PM (2016, 2017 and 2018)  
321 and PF (2017), the peak marker is the same, Rh12GR\_56601\_1304 (29.7 cM, located  
322 on chr6 at 31,814,891 bp). For PF2018, the peak marker is Rh88\_37299\_454 (11.5 cM,  
323 located on chr6 at 5,410,244 bp). These QTLs explained between 5.28 and 8.45% of  
324 the observed variance. The common 0.95 credible interval was from 15.59 to 42.49 cM,  
325 which covered from 8,578,645 to 44,264,630 bp on the physical map (Figure 4b, Table  
326 2).

327 On LG1, QTLs were only detected on the male map for PF for two years (2016 and  
328 2018), and explained 6.52 and 6.99% of phenotypic variance, respectively. The  
329 common 0.95 credible interval was at 12.78-44.11 cM, which covered from  
330 20,231,658-62,553,371 bp on the physical map (Figure 4b, Table 2).

331 We checked the interaction between OB3@Rh12GR\_16570\_782 and OB4@Rh12GR\_  
332 60129\_183, and between RW3@Rh12GR\_52506\_1218 and  
333 RW6@Rh12GR\_56601\_1304, and no significant interaction was detected.

### 334 *2.2 Two-part QTL analysis*

335 In order to extend the analysis even further, we performed a two-part QTL analysis to  
336 test the penetrance (presence/absence of prickles,  $LOD(p)$  were calculated with binary  
337 traits) and the severity (density of prickles on stems with prickles,  $LOD(\mu)$  were  
338 calculated with non-zero quantitative phenotype) of these QTLs.

339 For the hypothesis  $LOD(p)$  on the female and male maps, we obtained a significant  
340  $LOD(p)$  on the LG3 for the two types of stem (PF and PM) and the three years (Figure  
341 3, Supplementary Table 2). The marker with the highest LOD score on the OB map is  
342 the same: Rw35C24 (SSR marker) located at 44.4cM (Chr03: 40,215,502 bp). This  
343 QTL explained 13.38% to 16.72% of the variation. The peak marker on the RW map is  
344 also the same for PF and PM for the three years: Rh12GR\_52506\_1218 located at 42.6  
345 cM (42,317,122 bp). This QTL explained 20.69 to 33.21% of the variation. These data  
346 suggested that the QTL detected on LG3 mainly controls the presence/absence of  
347 prickles. Moreover, the  $LOD(p)$  on LG2 and LG6 for the male map were only  
348 significant in PF2016 and PM2016, respectively (Figure 3), and they showed a weak  
349 effect with an explanation of 1.80% and 2.70% of the variance, respectively  
350 (Supplementary Table 2).

351 For the  $LOD(\mu)$  hypothesis, we detected a significant QTL on the female map on LG4  
352 for PM (2016 and 2017) and PF (2016) (Figure 3, Supplementary Table 2). The QTLs

353 explained 9.02% to 9.88% of the observed phenotypic variances. Therefore, this QTL  
354 might be involved in the control of prickle density. On LG3, a significant QTL was  
355 detected on the male map for PM (2016, 2017, 2018) and PF (2016), suggesting that a  
356 QTL on LG3 might also control prickle density. This QTL is in the same region of the  
357 QTL detected for penetrance (Figure 3, Supplementary Table 2). On LG1, the LOD( $\mu$ )  
358 peaks in OB (PM2018) and in RW (PF2018) were higher than the genome-wide  
359 threshold ( $\mu$ ); these QTLs explained 6.66% and 7.80%, respectively, of prickle density  
360 variation.

### 361 2.3- The interaction of the LG3-QTL allele between OB and RW

362 Based on non-parametric and two-part methods, we identified QTLs for the presence  
363 of prickles on LG3 for the OB and RW maps in the same region. To further investigate  
364 how the alleles on these QTLs affect the presence of prickles, we visualized the number  
365 of prickles for each genotype in the hybrid population depending of the Mendelian  
366 distribution of the SNP markers at the LOD peak (Figure 5). The female and male  
367 alleles are referred to as  $a,b$  and  $c,d$ , respectively. The separation ratio  $ac:ad:bc:cd$  in  
368 offspring is 33:54:16:48, and was significantly different from the expected segregation  
369 of 1:1:1:1 (37.5 for each) with a  $p$ -value = 0.004 estimated by a chi-squared test (Figure  
370 5).

371 For PF and PM in all three years, we clearly see that the  $bd$  allele combination in hybrids  
372 is correlated with no-prickle individuals or individuals with only a few prickles (less  
373 than two on four internodes), whereas  $ac$ ,  $ad$  and  $bc$  genotypes present prickles (Figure  
374 5). These results suggest a dominant/recessive model for this QTL with the  $b$  and  $d$

375 alleles linked to the null or recessive alleles (prickless mutant) and the *a* and *c* alleles  
376 linked to the dominant alleles (prickles). For PM, a co-dominant effect can be detected  
377 since the phenotype for *ac* is significantly different from the one for *ad* and *bc* ( $ac > ad$   
378 and  $ac > bc$ ,  $p\text{-value} < 0.05$ , except for PM2016 between *ac* and *ab*; Figure 5), even if  
379 the effect is weak (no large difference between the mean for *ac* and *ad/bc*). For PF, no  
380 co-dominant effect was detected.

381 We also observed some odd phenotypes. For instance, OW9067 and OW9068 (red dots)  
382 had no prickles and were grouped in the *ad* genotype, perhaps due to recombination  
383 between the marker and the prickle locus (Figure 5). For individuals with the *bd*  
384 genotype, six individuals (blue and green dots) always have prickles: OW9062,  
385 OW9021, OW9052 and OW9109 (blue dots) look like the usual prickle genotypes and  
386 are probably caused by recombination, but the two extreme exceptions, OW9106 and  
387 OW9107 (green dots) with the highest prickle density are not that easy to clarify.  
388 Moreover, some individuals exist with both prickly and glabrous stems in the same  
389 plant.

### 390 **3- Candidate genes in the QTL interval region and gene expression analysis**

#### 391 *3.1 Candidate gene characterization and location in rose.*

392 Since it was proposed that prickles originate from a deformation of glandular trichomes  
393 in rose (Kellogg et al. 2011), we looked for rose homologues of transcription factors  
394 (TF) known to be involved in the molecular control of trichome initiation and  
395 development in Arabidopsis. The information from 15 TFs such as the bHLH (basic  
396 helix-loop-helix), C2H2 Zinc-Finger, MYB, WD40 repeat and WRKY families are

397 presented in Supplementary Table 3. For a more detailed annotation, we performed  
398 phylogenetic analyses on these protein families (Supplementary Figure 3).

399 Concerning the bHLH family (Supplementary Figure 3a), RC7G0190300,  
400 RC1G0342400 and RC6G0407800 showed strong similarity with GLABROUS3,  
401 MYC1 and TT8, respectively, where all of the proteins are in the same clade. They are  
402 referred to as RcGL3, RcMYC1 and RcTT8, respectively.

403 For the C2H2 family, RC3G0150000, RC4G0390900 and RC4G0476500 are closely  
404 related to GLABROUS INFLORESCENCE STEMS proteins (GIS, GIS2 and GIS3)  
405 and ZINC FINGER PROTEIN (ZFP5, 6 and 8). RC3G0150000 seems to be more  
406 closely related to GIS2, RC4G0390900 to GIS3 and RC4G0476500 to ZFP5.  
407 RC2G0415300 and RC6G0454700 are related to ZFP1 and ZFP3 and AT5G10970.  
408 They are referred to as RcZFP1-like1 and RcZFP1-like2, considering that they are  
409 closer to ZFP1 (Supplementary Figure 3b).

410 R2R3 MYB and R3 MYB belong to the MYB family (Supplementary Figure 3c). In  
411 the R2R3 MYB sub-family (blue sub-tree), RC7G0156100 is in the same clade as  
412 GLABROUS1, whereas RC2G0033100 and RC7G0261400 are more closely related to  
413 MYB82 and TT2, respectively. RC3G0322900 is in the same clade as MYB61, MYB50  
414 and MYB86. In the R3 MYB sub-family (red sub-tree), RC2G0548400, RC1G0560100  
415 and Chr1g0359121 (Raymond et al. 2018) are in the same clade of CPC, TRY, ETC1  
416 and ETC3. RC1G0560100 and Chr1g0359121 are more closely related to TRY and  
417 CPC, and are referred to as RcTRY and RcCPC, respectively. (Supplementary Figure  
418 3d).

419 In the WD40 family, RC1G0586100 showed a strong similarity to TRANSPARENT  
420 TESTA GLABRA 1(TTG1), and RC3G0186600 and RC2G0693200 also belong to this  
421 clade.

422 In the WRKY family, as previously shown by Hibrand-Saint Oyant et al. (2018),  
423 RC3G0244800 shows a strong similarity with AtTTG2 (TESTATRANSPARENT  
424 GLABRA2), whereas RC3G0309600 and RC3G0309700 seem to be more closely  
425 related to WRKY54 and WRKY70, RC3G0392200 to WRKY74, and RC3G0414600  
426 appears to be related to WRKY34 and WRKY2.

427 We then located these rose homologue genes on the rose genome and looked for co-  
428 location between these genes and the QTLs previously described (Figure 4A and B).

429 Concerning the QTLs on LG3 (male and female map, Figure 4a and b), the most  
430 interesting TF among the detected genes was *RcMYB61* (*RC3G0322900*, at Chr03:  
431 39,896,892-39,899,077) located in the cQTL interval (36.517-46.440 Mb) for the  
432 female map (Figure 4A). As previously described (Hibrand-Saint Oyant et al. 2018), a  
433 homologue of *TTG2*, a WRKY transcription factor (*RC3G0244800*), is also located in  
434 the credible interval. *RcGIS2* (*RC3G015000*), a *GIS2* homologue is also located on LG3  
435 but not in the cQTL interval. In addition to the candidate TFs, we also scanned the other  
436 TFs co-located in the cQTL interval on LG3 of the female map. There are four bHLH,  
437 two C2H2, three R2R3MYB and seven WD40 transcription factors (Supplementary  
438 Figure 3, in blue) located under the cQTL.

439 Concerning the cQTL interval on LG4, *RcGIS3* is positioned at Chr04: 50,315,805 -  
440 50,317,009 (1.21 Kb), and near the peak marker Rh12GR\_55601\_1304 (52,239,028

441 kb) on the female map (Figure 4A). *RC4G0476500*, a ZFP5 homologue, is also located  
442 on the female LG4 but not in the QTL interval.

443 Concerning the QTL on the male LG1, *RcMYC1*, *RcTRY* and *RcCPC*, which are  
444 positioned at 44,468,298-44,473,643 bp, 47,708,966-47,709,896 bp and 62,070,383-  
445 62,072,848 bp, respectively, are located in the cQTL region (20.232Mb-62.553Mb) of  
446 PF (2016, 2018) on the male LG1. The gene *RC1G0586100* (*RcTTG1*) is also located  
447 on LG1 but outside this interval.

448 For the male LG6, *RC6G0407800*, a homologue of *TT8*, is not located in the cQTL  
449 credible interval, and no studied gene was detected below this QTL.

### 450 *3.2 Candidate gene expression in glabrous and prickly roses.*

451 Based on the positional approach, we identified ten interesting candidate genes, six  
452 within the QTL interval and the other four outside of QTL but near the credible interval  
453 (Figure 4). In order to obtain more information about these genes, we studied their  
454 transcript accumulation by RT-qPCR in tissues from prickly (P) and prickless (NP)  
455 stems at different developmental stages: I, IIa, IIb, IIc, III (Supplementary Figure 1).

456 The cluster analysis of gene expression clearly showed that all the samples can be  
457 divided into two main groups: PI, NPI, PIIa, NPIIa, PIIb, NPIIb were gathered into one  
458 group, and PIIC, NPIIC, PIII, NPIII into another group (Figure 6a). At the sup-group  
459 level, PI and NPI, PIIa and NPIIa, PIIb and NPIIb, PIIC and NPIIC were clustered  
460 together, respectively. At the same stem developmental stage, prickly and glabrous  
461 samples (P and NP) behave similarly, suggesting no major difference of transcript  
462 accumulation between prickly and glabrous samples; the observed differences are more

463 closely related to stem development.

464 To extend the analysis even further, we used NP as a control to compare the normalized  
465 expression of genes between P and NP samples in the different stages (Figure 6b). In  
466 stage I, two genes are differentially expressed: *RcMYB61* and *RcGIS2* were down-  
467 regulated in prickly stems, with a significant p-value =  $4.1 \times 10^{-5}$  and  $2.9 \times 10^{-4}$  (Figure 6b),  
468 respectively. In stage IIa, only *RcZFP5* was significantly differentially expressed  
469 between P and NP, with a p-value = 0.0056 and FC = -5.7606 (Figure 6b). A different  
470 pattern is observed in stage IIb where *RcZFP5* expression was up-regulated with FC =  
471 8.2240 and a p-value = 0.0025. In addition, the transcripts of *RcMYC1*, *RcCPC* and  
472 *RcGIS2* were also significantly accumulated (p-value =  $4.1 \times 10^{-5}$ , 0.0048, 0.0012,  
473 respectively) in stage IIb. In stage IIc, no significant change in gene expression was  
474 detected. In stage III, the *RcGIS2* transcript is differentially accumulated with FC = -  
475 4.908 and a p-value = 0.043. The same pattern is observed for *RcMYB61* with a p-  
476 value =  $4.9 \times 10^{-4}$ .

477 We followed the transcript accumulation during stem development in prickly and  
478 glabrous stems (NPI as a control; Figure 6c). All the studied genes are regulated  
479 between the different samples. For instance, *RcMYB61* is up-regulated and *RcMYC1* is  
480 down-regulated between the different stages. For *RcZFP5*, we observed a delay in the  
481 decrease of transcript accumulation, with a decrease in stage IIa for glabrous stems and  
482 in stage IIb for stems with prickles (Figure 6c).

## 483 **Discussion**

484 *Two types of prickles are present in the OW progeny, originating from different*

485 *structures.*

486 A good understanding of prickles morphology is required to serve as the foundation for  
487 genetic and molecular studies. We identified two different types of prickles in our  
488 population: it appears that GP and NGP originate from glandular and non-glandular  
489 structures, respectively. This conclusion is different from previous studies in rose,  
490 which reported that prickles were extensions or modifications of glandular trichomes  
491 (Kellogg et al. 2011), and in other species (Ma et al. 2016b; Pandey et al. 2018). Asano  
492 et al. (2008) observed two types of prickles in the cultivated rose 'Laura', described as  
493 large size and small size prickles. The large size prickles look similar to NGPs in our  
494 study. The small size prickles, referred to as acicles (Asano et al. 2008), are more  
495 closely related to the glandular prickles (GP) we observed since they have a glandular  
496 head that accompanies them throughout their lifetime. The difference between these  
497 two types of prickles is also related to their segregation in the OW population (Figure  
498 1d), demonstrating that different genetic determinisms are involved. In this study, since  
499 only a few F<sub>1</sub> individuals had GPs, we cannot perform a genetic analysis on GPs, we  
500 concentrated our analysis on NGPs.

#### 501 *A complex genetic determinism for prickles in rose*

502 Prickles on stems exhibited transgressive segregation in diploid OW, the same as for  
503 the tetraploid K5 population (Koning-Boucoiran et al. 2012; Gitonga et al. 2014;  
504 Bourke et al. 2018), supporting the hypothesis that multiple loci may be responsible for  
505 this trait.

506 Using the ‘non- parametric’ QTL approach, we detected a stable QTL on LG3 in the  
507 three different years for both types of stems (PM and PF) on both the male and female  
508 genetic maps. We also demonstrated that this QTL mainly controls the  
509 presence/absence of prickles (Figure 3) using the ‘two-part’ QTL method. Interestingly,  
510 for PM in males, the QTL on LG3 may also be involved in regulating prickle density  
511 (severity in the two-part QTL analysis; Figure 3). A similar phenomenon was observed  
512 for the petal number with a locus on LG3 that controls the difference between simple  
513 and double petals, and a variance of the petal number that exists within the double petal  
514 flower is controlled by another locus (Roman et al. 2015; Hibrand-Saint Oyant et al.  
515 2018).

516 We further enhanced the description of QTLs on LG3 that affect the presence/absence  
517 of prickles. A significantly distorted segregation was observed at the peak marker  
518 position. That unusual segregation ratio might be explained by the presence of a self-  
519 incompatibility locus (Hibrand-Saint Oyant et al. 2018) near the peak marker for this  
520 QTL. On the basis of the phenotype-genotype relationship (Figure 5), we proposed that  
521 the *PRICKLE* alleles on this QTL are both heterozygous (np/P) in OB and RW, and that  
522 the presence of prickles is controlled by a dominant allele (np/P or P/P), and that the  
523 glabrous stem in the progeny is due to the combination of the two recessive alleles  
524 coming from both parents (np/np). These results are important for breeders who need  
525 to combine recessive alleles to obtain glabrous roses, an allelic combination that can be  
526 difficult in tetraploid roses. Development of specific molecular markers of the recessive  
527 allele may be useful for breeders. However, it should be noted that the actual markers

528 used (peak of the QTL) are only closely linked to the *PRICKLE* locus and few  
529 recombinants are observed in the progeny. Furthermore, the phenotype of the  
530 individuals with the two recessive alleles (*bd* phenotype; Figure 5) are not stable and  
531 some of the hybrids were regularly seen to develop some prickles on parts of the stems.  
532 Indeed, this phenomenon is widespread in roses. Rose breeders have reported that  
533 glabrous mutants have either been unstable for the prickless trait (Nobbs 1984; Rosu et  
534 al. 1995), or reverted to the prickly character after a freezing winter or other  
535 environmental stresses (Nobbs 1984; Oliver 1986; Druitt and Shoup 1991; Canli 2003).  
536 Taken together, we assumed that a single major locus on LG3 controlled the  
537 absence/presence of stem prickles. Further investigations are necessary to more closely  
538 identify molecular markers (for molecular assisted breeding) and the mechanisms  
539 behind the instability.

540 In the *ac*, *ad* and *bc* genotypes, each genotype has a continuous quantitative trait,  
541 indicating that there are other loci responsible for prickle density variance. Other QTLs  
542 affecting quantitative traits were detected on LG4 in OB and on LG1 and 3 in RW (Two-  
543 part QTL analysis; Figure 3). The LG4 QTL has a strong effect on PM but a weak effect  
544 on PF. For the QTL on LG1, it only had a weak effect on PF and on PM in 2018. Those  
545 three loci are related to the density of prickles, indicating that there are multiple genes  
546 responsible for the density trait, and that those genes have a different effect on the  
547 different stems.

#### 548 ***Detected QTLs are conserved in the Rosa genus and the Rosidae subfamily***

549 Thanks to the link between genetic maps and reference genome sequences (Hibrand-

550 Saint Oyant et al. 2018), we were able to compare our results with previous genetic  
551 studies by associating genetic map markers.

552 A QTL was previously detected on LG3 in different diploid and tetraploid populations  
553 (Crespel et al. 2002; Linde et al. 2006; Koning-Boucoiran et al. 2012; Hibrand-Saint  
554 Oyant et al. 2018 ; Bourke et al. 2018), which is consistent with our results: a strong  
555 QTL on Chr3 with a high LOD value was detected in all of the environments (across  
556 and between years and types of stems). This demonstrated that Chr3 QTL is a robust  
557 QTL detected independently of ploidy and the environment, and is present in various  
558 genetic backgrounds.

559 Recently, three QTLs on LG3, 4 and 6 were detected in the tetraploid K5 population  
560 with a high density of SNPs genetic map (Bourke et al. 2018). Interestingly, the QTLs  
561 identified from the diploid (OW) were almost identical to tetraploid (K5) populations  
562 (LG3, 4 and 6), with the slight difference that we also detected a weak QTL on LG1,  
563 which was only significant in males for two of the years. This slight difference might  
564 be due to the genetic background of the parents of the K5 and OW populations. In  
565 fact, in K5 populations, one parent is prickly and the other glabrous, whereas in OW  
566 populations, both parents have prickles. Bourke et al. (2018) reported that two SNP  
567 markers, K7826\_576 (located on the Chr3: 37,706,920 pb) and K5629\_995 (located on  
568 the Chr4: 57,791,999 bp) are linked to the stem prickles trait. When compared with our  
569 results, K7826\_576 is located within our Chr3 cQTL interval region (36,517,224-  
570 46,440,369 bp; Figure 4), and K5629\_995 is very close to our Chr4 QTL interval  
571 (46,189,407-56,107,784 bp). These results suggest that QTLs detected on LG3 and 4

572 could be similar between OW and K5 progenies.

573 In *Rosaceae*, the genetic determinism of prickles was studied in raspberry (*Rubus*  
574 *idaeus*), where two QTLs were detected on LG4 and 6 (Molina-Bravo et al. 2014).  
575 Using synteny viewer tools (<https://www.rosaceae.org/synview/search>; Jung et al.  
576 2014), we checked the synteny. The region where the QTL is located on LG6 in *R.*  
577 *occidentalis* (position 6,028Mb) is syntenic with a region on rose chromosome 2  
578 (position 42,330 Mb), where no QTL for prickles density was detected in our study. The  
579 region where the QTL 4 is located (position 0.101 Mb) is syntenic with the region on  
580 rose chromosome 4 (position 58,768 Mb), very close to the main QTL we detected on  
581 this chromosome (Table 2). These results could suggest that the two QTLs in rose and  
582 raspberry might be syntenic and share a common evolutionary history. In another  
583 publication, Graham et al. (2006) identified the gene *H* that controls cane pubescence.  
584 The locus is mapped on LG2, which is syntenic with the rose LG6 where one of the  
585 QTLs is located, detected in *R. x wichurana*. However, no precise location is available  
586 to allow us to assume a possible common origin.

#### 587 ***Candidate gene below the QTL interval region***

588 Prickles are assumed to originate from a ‘trichome-like structure’. In order to find a  
589 putative candidate gene for the identified QTLs, we looked for homologue genes known  
590 to be involved in trichome initiation and development in Arabidopsis. We annotated 15  
591 rose TFs that, based on similarity, can be involved in trichome development in rose:  
592 RcGL1, RcMYB82, RcMYB61, RcCPC, RcTRY, RcGL3, RcTT8, RcMYC1, RcTTG1,  
593 RcTTG2, RcZFP5, RcGIS3, RcGIS2, RcZFP1 and RcGL2 (Table 3). Among them, a

594 few were below the detected QTLs: RcMYB61 and RcTTG2 below the QTL on LG3;  
595 RcGIS3 below the QTL on LG4; and RcCPC, RcTRY and RcMYC1 below the QTL on  
596 LG1. ZFP5 (Chr04: 57,125,905 bp) is out of the QTL interval on LG4 in OW, but close  
597 to the peak LOD marker K5629\_995 of QTL in the K5 population (Chr04: 57,791,999  
598 bp) (Bourke et al. 2018). These genes are good candidates for the detected QTLs.

### 599 *Candidate genes transcript expression in glabrous and prickly F<sub>1</sub> individuals*

600 We quantified ten TF gene transcripts in glabrous and prickly F<sub>1</sub> individuals in different  
601 developmental stages using RT-qPCR. Surprisingly, minor differences were observed  
602 between glabrous and prickly samples, with the main differences occurring between  
603 developmental stages (as demonstrated by the heatmap analysis, Figure 6a). Based on  
604 transcript accumulation, this suggests that these homologues, known to be involved in  
605 trichome initiation and development in Arabidopsis, are not implicated in prickly  
606 initiation in rose, leading to the hypothesis that the two processes (trichome initiation  
607 and prickly initiation) might involve different gene pathways. The candidate gene  
608 approach may not be appropriate and a non-a priori approach such as a transcriptomic  
609 analysis could be done between individuals with and without prickles.

610 Nevertheless, some differences in transcript accumulation are observed between  
611 candidate genes. In the early stage (stage I), only *RcMYB61* and *RcGIS2* are slightly  
612 more highly accumulated in glabrous stems. However, GIS2 and MYB61 are positive  
613 regulators of trichome initiation (Gan et al. 2006), which is difficult to reconcile with  
614 an increase in transcript accumulation in glabrous stems (Figure 6). Negative feedback

615 regulation during prickle initiation can explain this point, as regularly observed in  
616 trichome initiation (Pattanaik et al. 2014) or, perhaps, differences are not at the  
617 transcriptional level. It could be interesting to sequence the genes in the two parents to  
618 see if a mutation can explain the phenotype.

619 *RcZFP5* may also be an interesting candidate gene. This gene showed a different  
620 regulation between glabrous and prickly stems. At stage IIa, *RcZFP5* shows a strong  
621 down-regulation in glabrous tissue, whereas this down-regulation is observed later at  
622 stage IIc in tissues with prickles (Figure 6C). Furthermore, this gene is close to the QTL  
623 on LG4. Its early repression in glabrous stems might explain why no prickles developed.  
624 In *A. thaliana*, *ZFP5* controls trichome initiation through GA signaling (Zhou et al.  
625 2011). These data (concerning *ZFP5* and *MYB61*) might suggest an implication of GA  
626 in prickle development. However, this hypothesis needs to be functionally validated in  
627 rose.

## 628 **Conclusion**

629 Prickle structure is an undesirable trait, not only in rose but in most crops in general.  
630 We identified a complex genetic determinism with a major locus on LG3 that controls  
631 the presence of prickles and a few QTLs that control prickle density. Further studies are  
632 necessary to develop markers for breeding selection and to identify the molecular bases.  
633 Using a candidate gene approach, we proposed different hypotheses concerning the  
634 gene involved in prickle initiation in rose. Approaches such as transcriptomics may help  
635 to identify new key regulators of prickle initiation and development in rose.

636 **Acknowledgements**

637 We are grateful to the experimental unit (UE Horti) for their technical assistance in  
638 plant management, and the ImHorPhen team (D. Besnard, R. Gardet) of IRHS for  
639 taking care of the plant cuttings in the greenhouse. We would also like to thank the  
640 IMAC technical platforms (F. Simonneau, A. Rolland) of SFR Quasav for supervising  
641 the histological experiment, and the PTM ANAN (M. Bahut) of the SFR Quasav for  
642 overseeing the RT-qPCR experiment. We acknowledge J. Chameau of the GDO team  
643 for helping to obtain the different stages of the sample.

644 This work was supported by funding from the National Natural Science Foundation of  
645 China (31760585), the China Scholarship Council ([2017]3109) and the Natural  
646 Science Foundation of Yunnan (2016FB061).

647 **Figure legends**

648 **Figure 1** Different types of prickles on the OW progeny stem and their distribution. **(a)**  
649 Stem prickles in the female ‘Old Blush’ (OB) and the male *R. x wichurana* (RW); NGPs:  
650 non-glandular prickles. **(b)** Stem prickles in F<sub>1</sub> progeny. Glabrous: no prickles  
651 whatsoever on the recorded stems in the three years. **(c)** Macroscopic photos of the  
652 terminal part of the stems with different types of prickles (number of offspring); GPs:  
653 glandular prickles. **(d)** The distribution and Q-Q plot of NGPs and GPs in the F<sub>1</sub>  
654 progeny in 2018; PF: prickles on the floral stem; PM: prickles on the main stem.

655 **Figure 2** LOD curves of the QTL scan for the NGPs on the floral (FM) and main (PM)  
656 stems in **(a)** female (OB) and **(b)** male map (RW) calculated with a non-parametric  
657 model for the three years (2016, 2017 and 2018, with red, blue and green lines,

658 respectively). The LOD threshold value is represented by a dotted line in red, blue and  
659 green for 2016, 2017 and 2018, respectively.

660 **Figure 3** LOD curves of the QTL scan for the NGPs on the floral (FM) and main (PM)  
661 stems in (a) female (OB) and (b) male (RW) maps calculated using the two-part  
662 approach. The LOD (p) value (penetrance) is in red, the LOD ( $\mu$ ) value (severity) is in  
663 blue, and the LOD (p,  $\mu$ ) value is in black. The dotted line represents the LOD threshold.  
664 QTLs above threshold value are indicated by stars: red for penetrance, blue for severity.

665 **Figure 4** Common QTLs (cQTLs) and candidate genes in (a) the female linkage groups  
666 3 and 4, and (b) the male linkage groups 1, 3 and 6. Areas highlighted in pink, blue and  
667 yellow on the linkage groups represent the 0.95 Bayesian interval of cQTL for specific  
668 PF, PM and both, respectively. Bars and lines on the right of each chromosome  
669 represent 0.95 and 0.99 Bayesian intervals of the QTL with a different color for NGPs  
670 on the floral stem and the main stem (pink and blue, respectively). The red markers are  
671 the peak of the QTL. Brown markers are SSR markers and black markers are SNP  
672 markers.

673 **Figure 5** The interaction of the different alleles of the LG3 QTL between OB and RW.  
674 Genotype: *ac*, *ad*, *bc*, *bd* (number of individuals), *a/b* and *c/d* alleles belong to females  
675 and males, respectively. For the phenotype, the mean values of prickly density for PF  
676 and PM for the three years are presented. Some individuals are highlighted with green  
677 dots (OW9106 and OW9107), blue dots (OW9062, OW9021, OW9052 and OW9109)  
678 and red dots (OW9067 and OW9068). The asterisk indicates that the difference is  
679 significant with a p-value of less than 0.05

680 **Figure 6** Transcript accumulation of candidate genes followed by qPCR during prickle  
681 development. **(a)** A heatmap of samples and genes. **(b)** The scatter plot of the candidate  
682 genes' normalized expression in prickle and glabrous individuals in different stages (as  
683 defined in Supplementary Figure 1). The red and green lines represent a two-fold  
684 change in the accumulation with an increase or a decrease, respectively. Gene  
685 transcripts differentially accumulated ( $p$ -value  $< 0.05$ ) are represented by red or green  
686 dots for up- or down-accumulation, respectively. **(c)** Transcript accumulation in the  
687 different stages of prickle (P) and glabrous (NP) stems with NPI as a control.

## 688 **Electronic Supplementary Material**

689 **Supplementary Figure 1** Stem development and sampling stages in (a) non-glandular  
690 prickles (NGP, OW9137), (b) glandular prickles (GP, OW9106), and (c) glabrous stems  
691 (NP, OW9068). For the glabrous stems, the developmental stages correspond to the  
692 stages for the stem with prickles.

693 **Supplementary Figure 2** Frequency distribution and Q-Q plot of non-glandular  
694 prickles on four internodes in the OW population for floral stems (PF) and the main  
695 stem (PM) for the three years (2016, 2017 and 2018).

696 **Supplementary Figure 3** Phylogenetic analysis of the transcription factor family  
697 involved in trichome initiation and development: (a) bHLH, (b) C2H2 Zinc-Finger, (c)  
698 MYB: R3MYB (red sub-tree) and R2R3MYB (blue sub-tree), and (d) WD40. The rose  
699 genes homologues of genes involved in trichome initiation and development are in red.  
700 For *A. thaliana*, the protein name corresponds to the TAIR database  
701 (<https://www.arabidopsis.org/>), and for rose, to the reference genome of the haploid of

702 ‘Old Blush’ (Hibrand-Saint Oyant et al. (2018)), except for Chr1g0359121 and  
703 Chr2g0138951 (Raymond et al. 2018).

704 **Supplementary Table 1** Primer sequences of candidate genes for qPCR

705 **Supplementary Table 2** Summary of QTLs for NGPs using the two-part QTL model  
706 in OW progeny

707 **Supplementary Table 3** Summary of the rose homologous genes known in *A. thaliana*  
708 to be involved in trichome initiation

709 **Supplementary Table 4** Prickle number on four internodes of two types of stems for  
710 the three years in OW progeny.

## 711 **References**

712 Asano G, Kubo R, Tanimoto S (2008) Growth, structure and lignin localization in  
713 rose prickles. Bull. Fac. Agr., Sagai Univ. 93:117–125

714 Balkunde R, Pesch M, Hülkamp M (2010) Chapter ten - trichome patterning in  
715 *Arabidopsis thaliana*: from genetic to molecular models. In: Timmermans  
716 MCP (ed) Current Topics in Developmental Biology. Academic Press, pp  
717 299–321

718 Bourke PM, Gitonga VW, Voorrips RE, et al (2018) Multi-environment QTL analysis  
719 of plant and flower morphological traits in tetraploid rose. Theor Appl Genet  
720 131:2055–2069. <https://doi.org/10.1007/s00122-018-3132-4>

721 Boyartchuk VL, Broman KW, Mosher RE, et al (2001) Multigenic control of *Listeria*  
722 *monocytogenes* susceptibility in mice. Nat Genet 27:259–260.  
723 <https://doi.org/10.1038/85812>

724 Broman KW (2003) Mapping quantitative trait loci in the case of a spike in the  
725 phenotype distribution. Genetics 163:1169–1175

726 Burns KC (2014) Are there general patterns in plant defence against megaherbivores?  
727 Biol J Linn Soc 111:38–48. <https://doi.org/10.1111/bij.12181>

728 Canli FA (2003) A review on thornless roses. Pak J Biol Sci 6:1712–1719

- 729 Canli FA, Kazaz S (2009) Biotechnology of roses: progress and future prospects.  
730 *Türkiye Orman Derg* 10:167–183
- 731 Canli FA, Skirvin RM (2003) Separation of thornless rose chimeras into their (*Rosa*  
732 *sp.*) consistent genotypes in vitro. *Pak J Biol Sci* 6:1644–1648
- 733 Chopra D, Mapar M, Stephan L, et al (2019) Genetic and molecular analysis of  
734 trichome development in *Arabis alpina*. *Proc Natl Acad Sci* 116:12078–  
735 12083. <https://doi.org/10.1073/pnas.1819440116>
- 736 Crespel L, Chirollet M, Durel C, et al (2002) Mapping of qualitative and quantitative  
737 phenotypic traits in *Rosa* using AFLP markers. *Theor Appl Genet* 105:1207–  
738 1214. <https://doi.org/10.1007/s00122-002-1102-2>
- 739 Debener T (1999) Genetic analysis of horticulturally important morphological and  
740 physiological characters in diploid roses. *Gartenbauwissenschaft* 64:14–20
- 741 Druitt L, Shoup M (1991) Thornless roses. *Horticulture*, 69:78-82.
- 742 Gan Y, Kumimoto R, Liu C, et al (2006) GLABROUS INFLORESCENCE STEMS  
743 modulates the regulation by gibberellins of epidermal differentiation and shoot  
744 maturation in *Arabidopsis*. *Plant Cell* 18:1383–1395.  
745 <https://doi.org/10.1105/tpc.106.041533>
- 746 Gan Y, Liu C, Yu H, Broun P (2007) Integration of cytokinin and gibberellin  
747 signalling by *Arabidopsis* transcription factors GIS, ZFP8 and GIS2 in the  
748 regulation of epidermal cell fate. *Development* 134:2073–2081.  
749 <https://doi.org/10.1242/dev.005017>
- 750 Gitonga VW, Koning-Boucoiran CF, Verlinden K, et al (2014) Genetic variation,  
751 heritability and genotype by environment interaction of morphological traits in  
752 a tetraploid rose population. *BMC Genet* 15:146.  
753 <https://doi.org/10.1186/s12863-014-0146-z>
- 754 Graham J, Smith K, Tierney I, et al (2006) Mapping gene *H* controlling cane  
755 pubescence in raspberry and its association with resistance to cane botrytis and  
756 spur blight, rust and cane spot. *Theor Appl Genet* 112:818–831.  
757 <https://doi.org/10.1007/s00122-005-0184-z>
- 758 Hibrand-Saint Oyant L, Ruttink T, Hamama L, et al (2018) A high-quality genome  
759 sequence of *Rosa chinensis* to elucidate ornamental traits. *Nat Plants* 4:473.  
760 <https://doi.org/10.1038/s41477-018-0166-1>
- 761 Huchelmann A, Boutry M, Hachez C (2017) Plant glandular trichomes: natural cell  
762 factories of high biotechnological Interest. *Plant Physiol* 175:6–22.  
763 <https://doi.org/10.1104/pp.17.00727>

- 764 Ishida T, Kurata T, Okada K, Wada T (2008) A genetic regulatory network in the  
765 development of trichomes and root hairs. *Annu Rev Plant Biol* 59:365–386.  
766 <https://doi.org/10.1146/annurev.arplant.59.032607.092949>
- 767 Jung S, Ficklin SP, Lee T, et al (2014) The Genome Database for *Rosaceae* (GDR):  
768 year 10 update. *Nucleic Acids Res* 42:D1237–D1244.  
769 <https://doi.org/10.1093/nar/gkt1012>
- 770 Kawamura K, Oyant LH-S, Crespel L, et al (2011) Quantitative trait loci for  
771 flowering time and inflorescence architecture in rose. *Theor Appl Genet*  
772 122:661–675. <https://doi.org/10.1007/s00122-010-1476-5>
- 773 Kellogg AA, Branaman TJ, Jones NM, et al (2011) Morphological studies of  
774 developing *Rubus* prickles suggest that they are modified glandular trichomes.  
775 *Botany* 89:217–226. <https://doi.org/10.1139/b11-008>
- 776 Kim SY, Hyoung S, So WM, Shin JS (2018) The novel transcription factor TRP  
777 interacts with ZFP5, a trichome initiation-related transcription factor, and  
778 negatively regulates trichome initiation through gibberellic acid signaling.  
779 *Plant Mol Biol* 96:315–326. <https://doi.org/10.1007/s11103-018-0697-x>
- 780 Kirik V, Lee MM, Wester K, et al (2005) Functional diversification of MYB23 and  
781 GL1 genes in trichome morphogenesis and initiation. *Development* 132:1477–  
782 1485. <https://doi.org/10.1242/dev.01708>
- 783 Koning-Boucoiran CFS, Dolstra O, van der Linden CG, et al (2009) Specific mapping  
784 of disease resistance genes in tetraploid cut roses. *Acta Hort* 836:137–142.  
785 <https://doi.org/10.17660/ActaHortic.2009.836.19>
- 786 Koning-Boucoiran CFS, Gitonga VW, Yan Z, et al (2012) The mode of inheritance in  
787 tetraploid cut roses. *Theor Appl Genet* 125:591–607.  
788 <https://doi.org/10.1007/s00122-012-1855-1>
- 789 Li H, Liu FL, Lin X, et al (2012) Studies on anatomical structure and chemical  
790 composition in prickles of *Rosa hybrida*. *Acta Hort* Sin 39:1321–1329
- 791 Linde M, Hattendorf A, Kaufmann H, Debener Th (2006) Powdery mildew resistance  
792 in roses: QTL mapping in different environments using selective genotyping.  
793 *Theor Appl Genet* 113:1081–1092. [https://doi.org/10.1007/s00122-006-0367-](https://doi.org/10.1007/s00122-006-0367-2)  
794 2
- 795 Ma D, Hu Y, Yang C, et al (2016a) Genetic basis for glandular trichome formation in  
796 cotton. *Nat Commun* 7:1–9. <https://doi.org/10.1038/ncomms10456>

- 797 Ma Z-Y, Wen J, Ickert-Bond SM, et al (2016b) Morphology, structure, and ontogeny  
798 of trichomes of the grape genus (*Vitis*, *Vitaceae*). *Front Plant Sci* 7:704.  
799 <https://doi.org/10.3389/fpls.2016.00704>
- 800 Maes L, Inzé D, Goossens A (2008) Functional specialization of the  
801 TRANSPARENT TESTA GLABRA1 network allows differential hormonal  
802 control of laminal and marginal trichome initiation in *Arabidopsis* rosette  
803 leaves. *Plant Physiol* 148:1453–1464. <https://doi.org/10.1104/pp.108.125385>
- 804 Matías-Hernández L, Jiang W, Yang K, et al (2017) AaMYB1 and its orthologue  
805 AtMYB61 affect terpene metabolism and trichome development in *Artemisia*  
806 *annua* and *Arabidopsis thaliana*. *Plant J* 90:520–534.  
807 <https://doi.org/10.1111/tpj.13509>
- 808 Molina-Bravo R, Fernandez GE, Sosinski BR (2014) Quantitative trait locus analysis  
809 of tolerance to temperature fluctuations in winter, fruit characteristics, flower  
810 color, and prickle-free canes in raspberry. *Mol Breed* 33:267–280.  
811 <https://doi.org/10.1007/s11032-013-9947-4>
- 812 Nobbs KJ (1984) American Rose Annual. In: Shreveport (ed) Breeding thornless  
813 roses. The American Rose Society, pp 37–43
- 814 Oliver WG (1986) A précis of thornless development. The rose. The Royal National  
815 Rose Society, 80(3).
- 816 Pandey S, Goel R, Bhardwaj A, et al (2018) Transcriptome analysis provides insight  
817 into prickle development and its link to defense and secondary metabolism in  
818 *Solanum viarum* Dunal. *Sci Rep* 8:1–12. [https://doi.org/10.1038/s41598-018-](https://doi.org/10.1038/s41598-018-35304-8)  
819 [35304-8](https://doi.org/10.1038/s41598-018-35304-8)
- 820 Patra B, Pattanaik S, Yuan L (2013) Ubiquitin protein ligase 3 mediates the  
821 proteasomal degradation of GLABROUS 3 and ENHANCER OF  
822 GLABROUS 3, regulators of trichome development and flavonoid  
823 biosynthesis in *Arabidopsis*. *Plant J* 74:435–447.  
824 <https://doi.org/10.1111/tpj.12132>
- 825 Pattanaik S, Patra B, Singh SK, Yuan L (2014) An overview of the gene regulatory  
826 network controlling trichome development in the model plant, *Arabidopsis*.  
827 *Front Plant Sci* 5:259. <https://doi.org/10.3389/fpls.2014.00259>
- 828 Pesch M, Dartan B, Birkenbihl R, et al (2014) *Arabidopsis* TTG2 regulates *TRY*  
829 expression through enhancement of activator complex-triggered activation.  
830 *Plant Cell* 26:4067–4083. <https://doi.org/10.1105/tpc.114.129379>

- 831 Pesch M, Hülskamp M (2004) Creating a two-dimensional pattern *de novo* during  
832 Arabidopsis trichome and root hair initiation. *Curr Opin Genet Dev* 14:422–  
833 427. <https://doi.org/10.1016/j.gde.2004.06.007>
- 834 Randoux M, Jeauffre J, Thouroude T, et al (2012) Gibberellins regulate the  
835 transcription of the continuous flowering regulator, *RoKSN*, a rose *TFL1*  
836 homologue. *J Exp Bot* 63:6543–6554. <https://doi.org/10.1093/jxb/ers310>
- 837 Raymond O, Gouzy J, Just J, et al (2018) The *Rosa* genome provides new insights  
838 into the domestication of modern roses. *Nat Genet* 50:772–777.  
839 <https://doi.org/10.1038/s41588-018-0110-3>
- 840 Rerie WG, Feldmann KA, Marks MD (1994) The *GLABRA2* gene encodes a homeo  
841 domain protein required for normal trichome development in Arabidopsis.  
842 *Genes Dev* 8:1388–1399. <https://doi.org/10.1101/gad.8.12.1388>
- 843 Roccia A, Oyant LH-S, Cavel E, et al (2019) Biosynthesis of 2-Phenylethanol in rose  
844 petals is linked to the expression of one allele of *RhPAAS*. *Plant Physiol*  
845 179:1064–1079. <https://doi.org/10.1104/pp.18.01468>
- 846 Roman H, Rapicault M, Miclot AS, et al (2015) Genetic analysis of the flowering date  
847 and number of petals in rose. *Tree Genet Genomes* 11:85.  
848 <https://doi.org/10.1007/s11295-015-0906-6>
- 849 Ronel M, Lev-Yadun S (2012) The spiny, thorny and prickly plants in the flora of  
850 Israel. *Bot J Linn Soc* 168:344–352. <https://doi.org/10.1111/j.1095-8339.2011.01211.x>
- 852 Rosu A, Skirvin RM, Bein A, et al (1995) The development of putative adventitious  
853 shoots from a chimeral thornless rose (*Rosa multiflora* Thunb. ex J. Murr.)  
854 *in vitro*. *J Hortic Sci* 70:901–907.  
855 <https://doi.org/10.1080/14620316.1995.11515365>
- 856 Shupert DA, Byrne DH, Brent Pemberton H (2007) Inheritance of flower traits, leaflet  
857 number and prickles in roses. *Acta Hort* 751:331–335.  
858 <https://doi.org/10.17660/ActaHortic.2007.751.42>
- 859 Symonds VV, Hatlestad G, Lloyd AM (2011) Natural allelic variation defines a role  
860 for *ATMYC1*: trichome cell fate determination. *PLOS Genet* 7:e1002069.  
861 <https://doi.org/10.1371/journal.pgen.1002069>
- 862 Traw MB, Bergelson J (2003) Interactive effects of jasmonic acid, salicylic acid, and  
863 gibberellin on induction of trichomes in Arabidopsis. *Plant Physiol* 133:1367–  
864 1375. <https://doi.org/10.1104/pp.103.027086>

- 865 Wang S, Chen J-G (2014) Regulation of cell fate determination by single-repeat R3  
866 MYB transcription factors in Arabidopsis. *Front Plant Sci* 05:133.  
867 <https://doi.org/10.3389/fpls.2014.00133>
- 868 Wang S, Hubbard L, Chang Y, et al (2008) Comprehensive analysis of single-repeat  
869 R3 MYB proteins in epidermal cell patterning and their transcriptional  
870 regulation in Arabidopsis. *BMC Plant Biol* 8:81. <https://doi.org/10.1186/1471-2229-8-81>  
871
- 872 Wester K, Digiuni S, Geier F, et al (2009) Functional diversity of R3 single-repeat  
873 genes in trichome development. *Development* 136:1487–1496.  
874 <https://doi.org/10.1242/dev.021733>
- 875 Young MA (2007) Modern roses 12: The comprehensive list of roses in cultivation or  
876 of historical or botanical importance. *Shreveport*: The American Rose Society
- 877 Zhang F (2003) A network of redundant bHLH proteins functions in all TTG1-  
878 dependent pathways of Arabidopsis. *Development* 130:4859–4869.  
879 <https://doi.org/10.1242/dev.00681>
- 880 Zhao H, Wang X, Zhu D, et al (2012) A single amino acid substitution in IIIf  
881 subfamily of basic Helix-Loop-Helix transcription factor AtMYC1 leads to  
882 trichome and root hair patterning defects by abolishing its interaction with  
883 partner proteins in Arabidopsis. *J Biol Chem* 287:14109–14121.  
884 <https://doi.org/10.1074/jbc.M111.280735>
- 885 Zhou Z, An L, Sun L, et al (2011) Zinc finger protein5 is required for the control of  
886 trichome initiation by acting upstream of zinc finger protein8 in Arabidopsis.  
887 *Plant Physiol* 157:673–682. <https://doi.org/10.1104/pp.111.180281>
- 888 Zhou Z, Sun L, Zhao Y, et al (2013) Zinc Finger Protein 6 (ZFP6) regulates trichome  
889 initiation by integrating gibberellin and cytokinin signaling in *Arabidopsis*  
890 *thaliana*. *New Phytol* 198:699–708. <https://doi.org/10.1111/nph.12211>
- 891

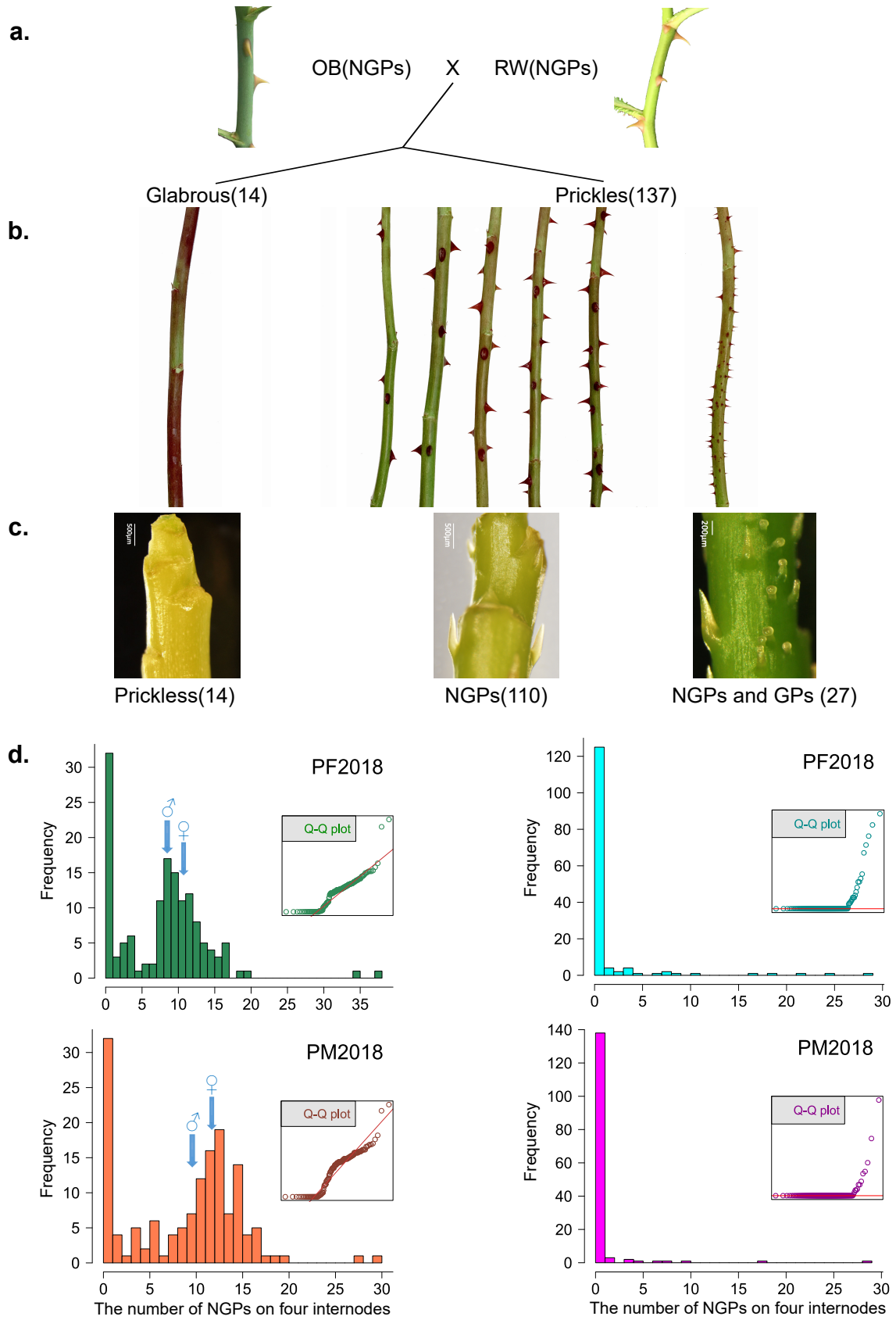


**Figure 1**

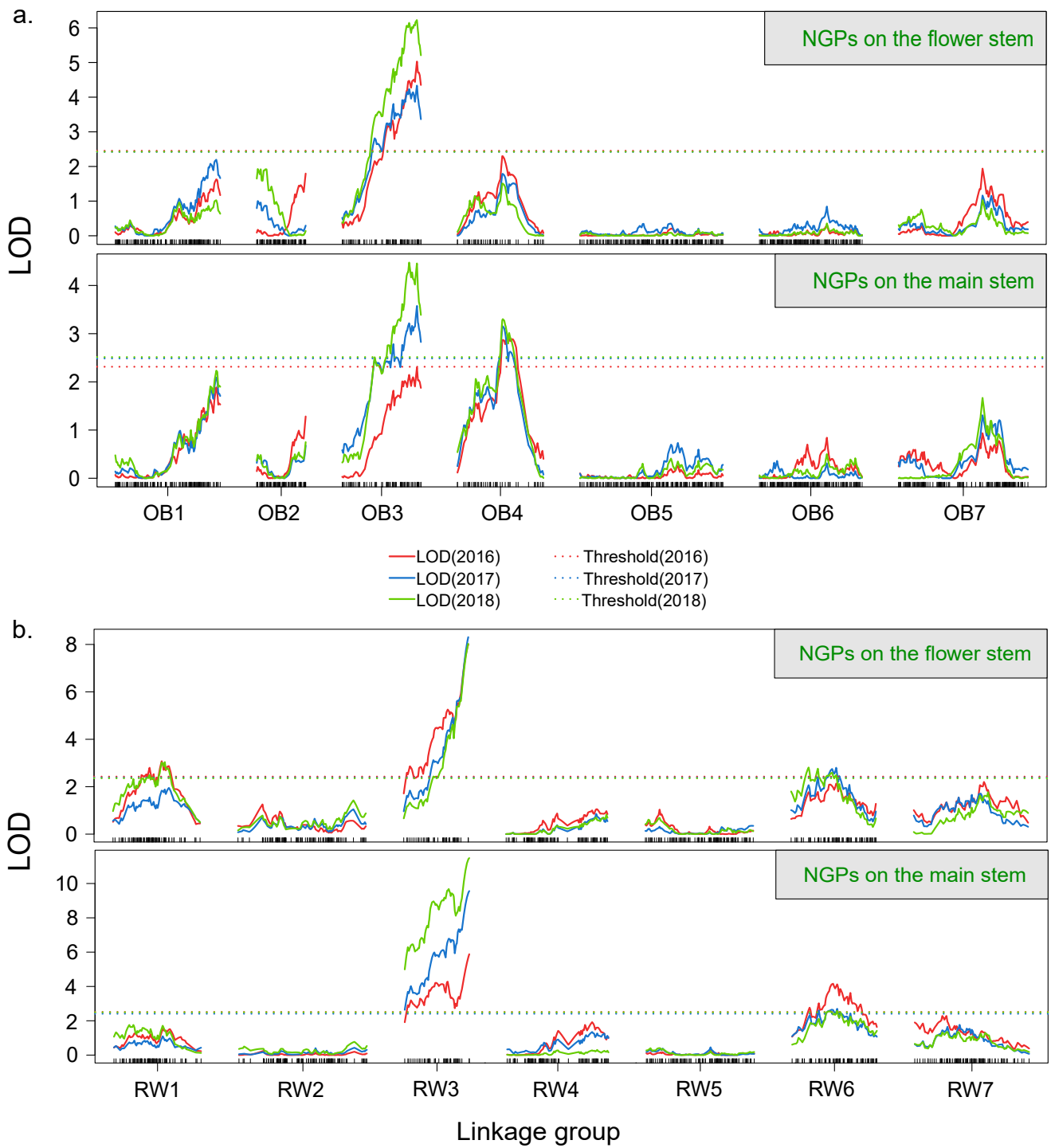


**Figure 2**

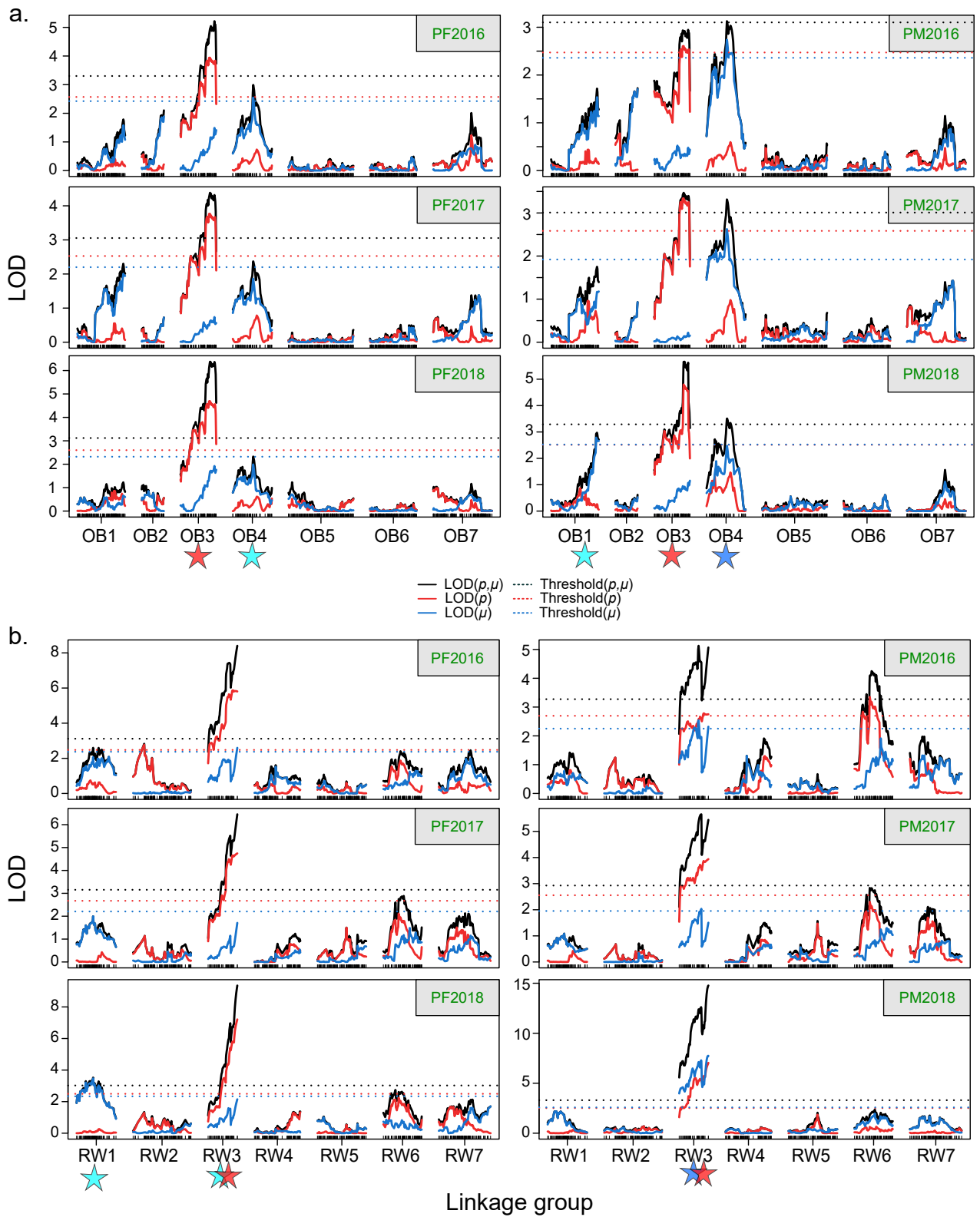


**Figure 3**



b.

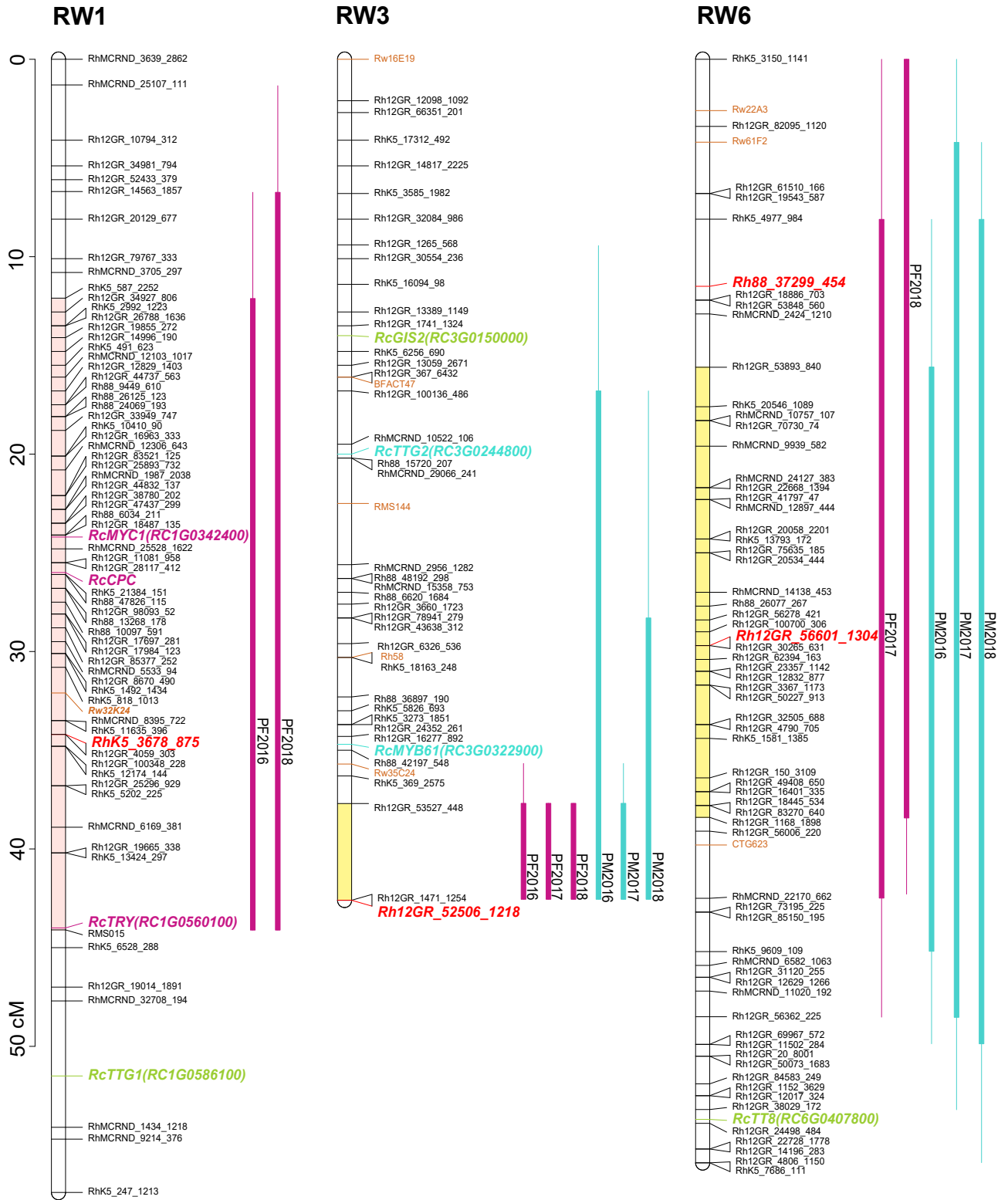
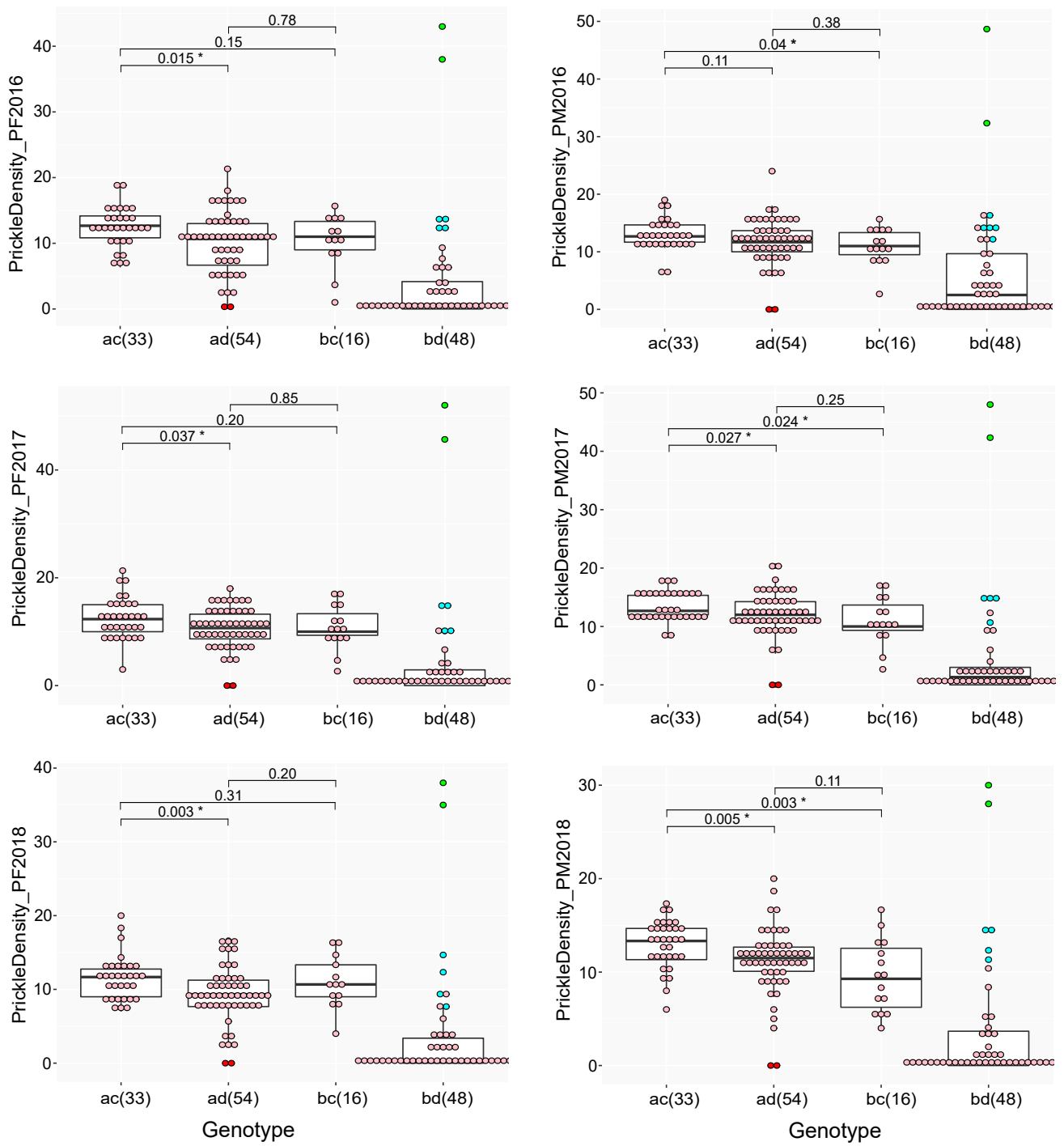
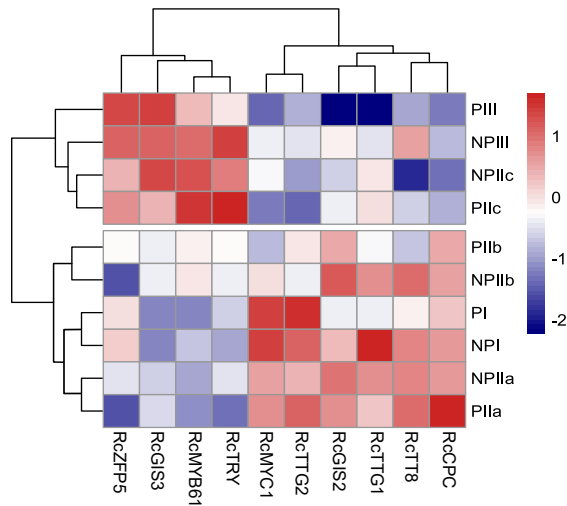


Figure 4

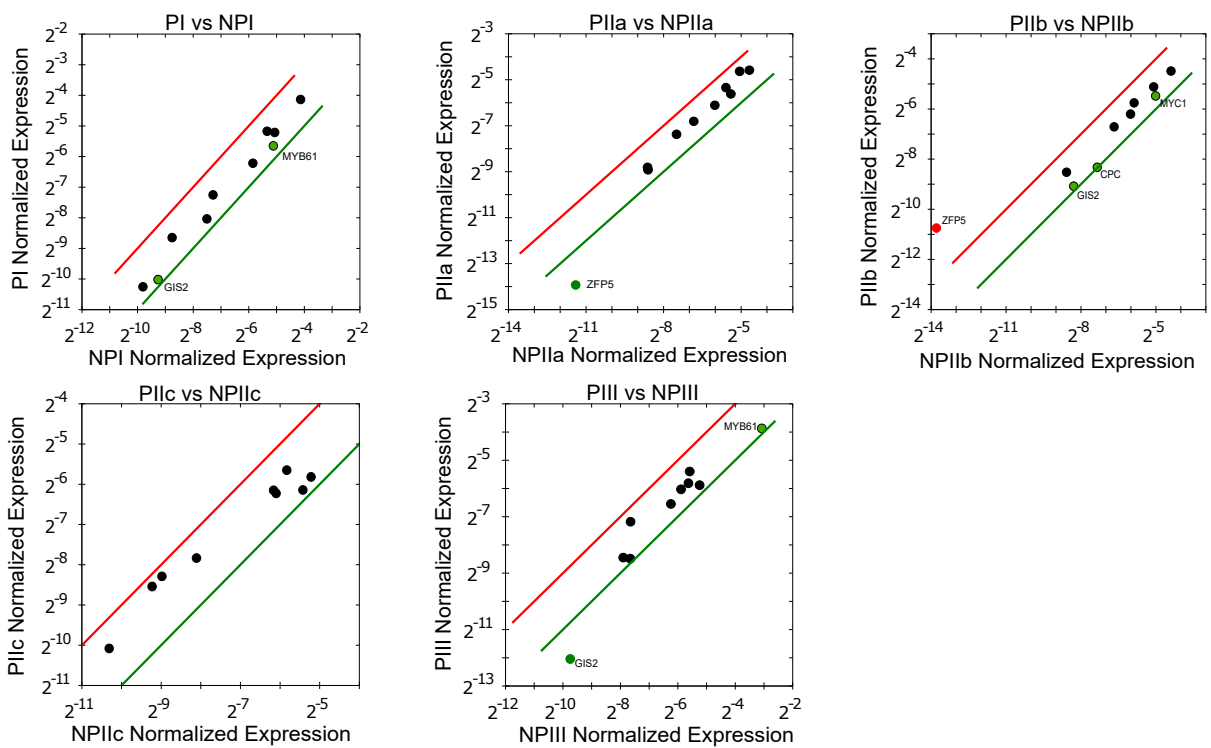


**Figure 5**

a.



b.



c.

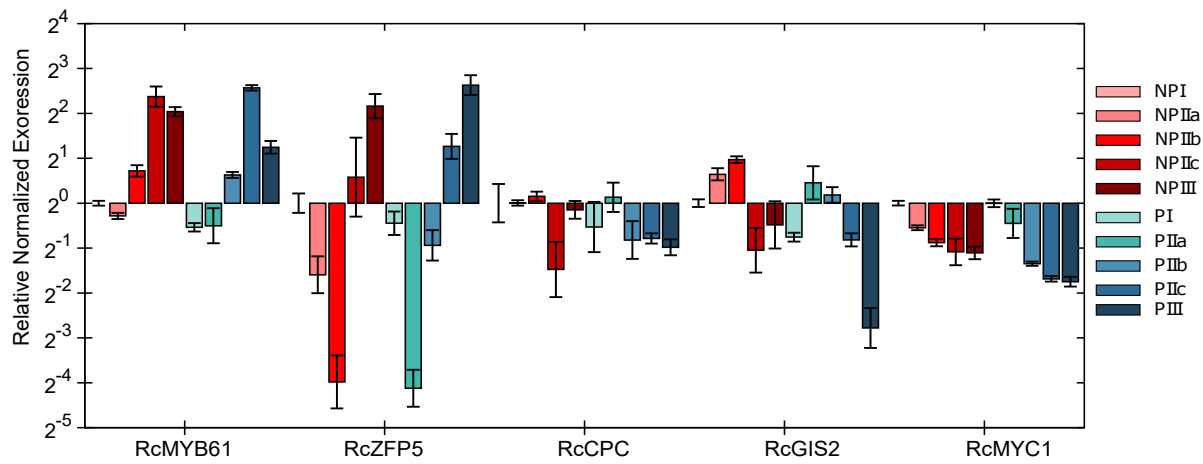


Figure 6

Table 1 Mean, median and range values for prickles on 4 internodes, phenotypic variance components and the trait heritability

Trait	Year	OB Mean±SD	RW Mean±SD	F1					Kruskal-Wallis test (p-value)				Variance comp					
				range	1st Qu	Mean	median	3rd Qu	Genotype	Replicate shoots	Year	Stem type	$\sigma^2_G$	SE <sub>G</sub>	$\sigma^2_{GY}$	SE <sub>GY</sub>		
PF	2016	11.3±1.3	8.9±0.8	0 - 43	2.4	8.5	9.8	12.7										
	2017	11.6±1.1	8.9±0.9	0 - 52	2.7	9.0	9.7	13.0	<2.20E-16 <sup>***</sup>	0.96 <sup>N</sup>	0.06 <sup>**</sup>							
	2018	10.6±1.0	8.4±0.5	0 - 38	2.7	7.9	9.0	11.3				4.93E-08 <sup>***</sup>	41.41	4.98	1.50	0.26		
PM	2016	11.9±1.6	9.3±1.2	0 - 48	6.7	10.2	11.7	13.3										
	2017	11.8±1.4	9.2±1.1	0 - 47	3.0	10.2	11.3	14.0	<2.20E-16 <sup>***</sup>	0.81 <sup>N</sup>	0.04 <sup>***</sup>							
	2018	11.7±1.6	9.1±1.1	0 - 30	3.5	8.8	10.8	13.0										

PF: prickles on the floral stem

PM: prickles on the main stem

1st Qu: First quartile(Q1) means 25% observations are below this quantity (approx)

3rd Qu: Third quartile(Q3) means 75% observations are below this quantity (approx)

$\sigma^2_G$ : Variance components of genotype, genotype x year interaction ( $\sigma^2_{GY}$ ), genotype x stem interaction ( $\sigma^2_{GS}$ ), and the residual error ( $\sigma^2_E$ )

SE: the standard error

$h^2$ : Narrow sense heritability

Component in $\sigma_p^2$				$h^2(\%)$	SE
$\sigma_{GS}^2$	SE <sub>GS</sub>	$\sigma_E^2$	SE <sub>E</sub>		

1.27 0.27 9.13 0.29 96.66 0.0048

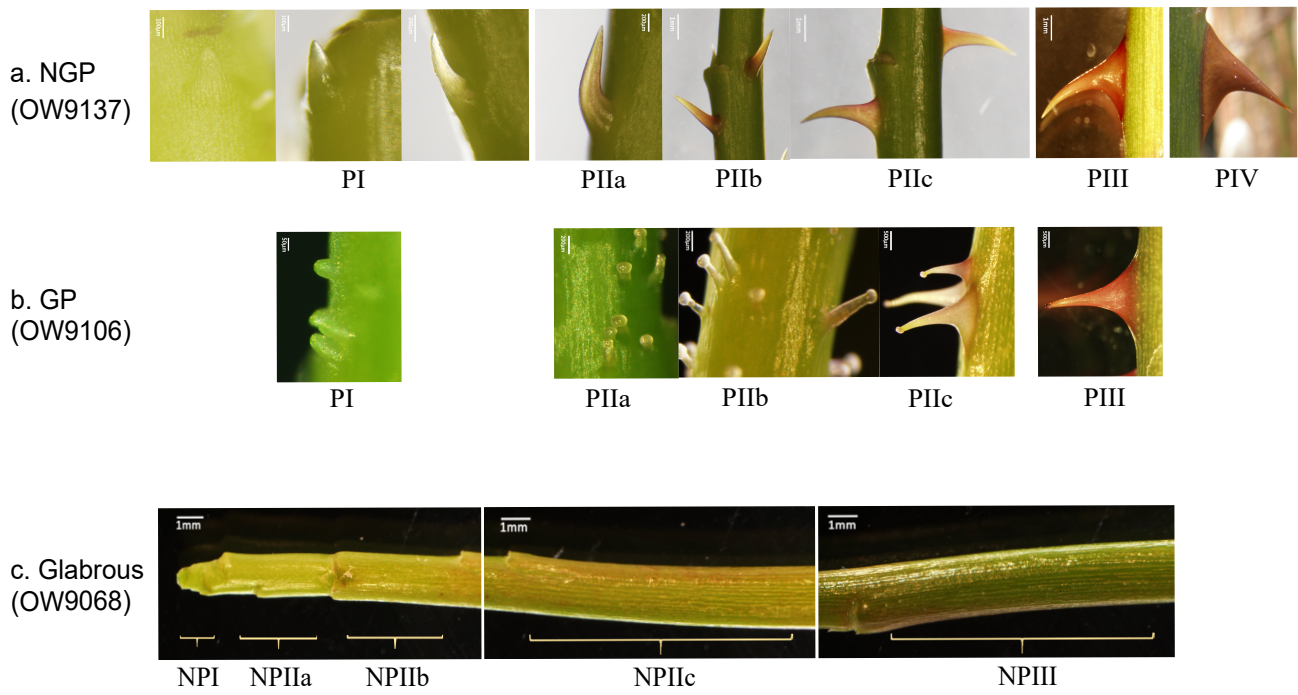
---

**Table 2 Summary of QTLs for NGP with non-parametric model in OW progeny**

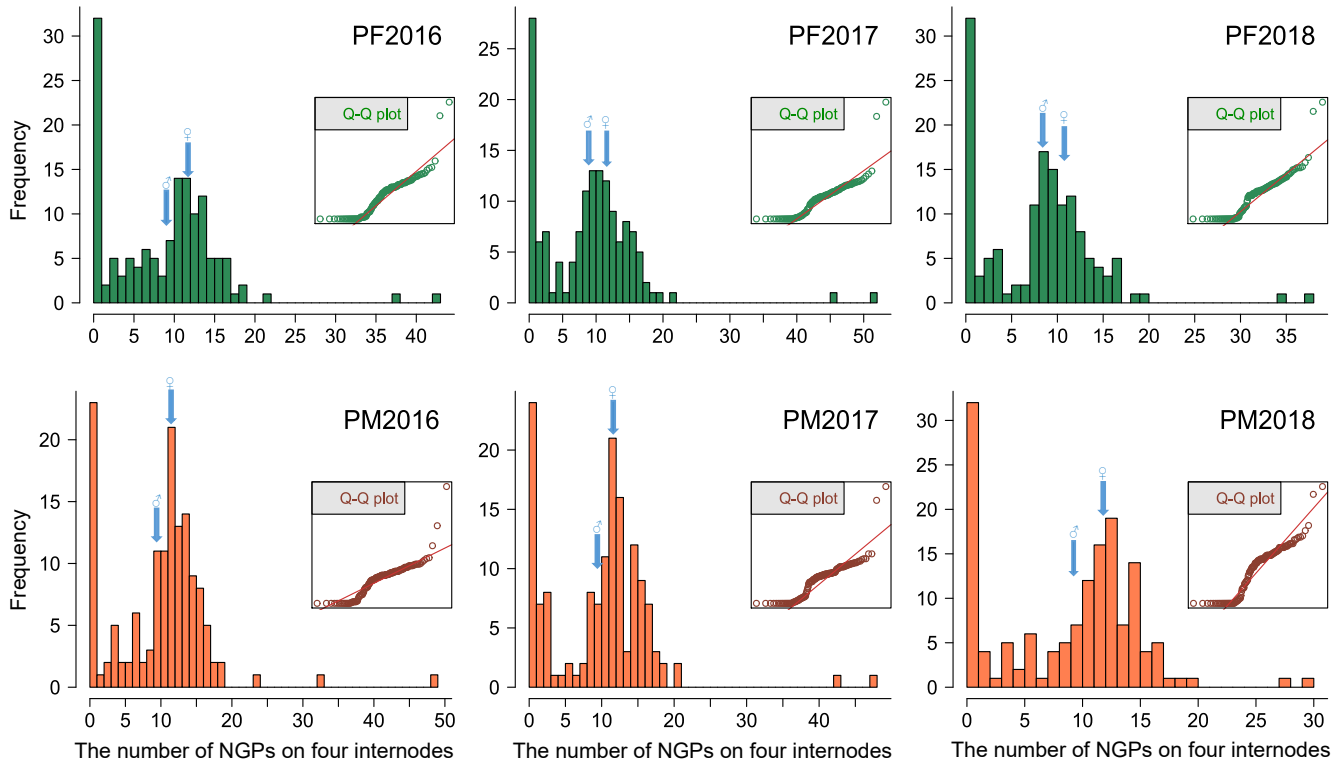
QTL	Phenotyping	PT <sup>a</sup>	QTL Characteristics					0.95 bayes interval		0.99 bayes interval	
			LOD	LG@positon <sup>b</sup>	r(%) <sup>c</sup>	MM <sup>d</sup>	bp <sup>e</sup>	cM <sup>f</sup>	bp	cM	bp
1a	PF2016	2.45	5.03	OB3@51.1	11.74	Rh12GR_16570_782	44459262	40.38 - 53.75	36517224 - 46440369	27.59 - 53.75	27934327 - 46440369
	PF2017	2.42	4.33	OB3@51.1	6.92	Rh12GR_16570_782	44459262	30.31 - 53.75	33612066 - 46440369	20.14 - 53.75	24888779 - 46440369
	PF2018	2.43	6.22	OB3@51.1	14.84	Rh12GR_16570_782	44459262	39.71 - 53.75	36517224 - 46440369	32.98 - 53.75	33612066 - 46440369
	PM2016	2.31	2.31	OB3@51.1	7.29	Rh12GR_16570_782	44459262	27.59 - 53.75	27934327 - 46440369	15.43 - 53.75	23585838 - 46440369
	PM2017	2.49	3.58	OB3@51.1	6.65	Rh12GR_16570_782	44459262	20.14 - 53.75	24888779 - 46474274	18.8 - 53.75	24000000 - 46440369
	PM2018	2.51	4.48	OB3@45.7	11.78	Rh12GR_34665_95	41401120	36.99 - 53.75	35014990 - 46440369	20.14 - 53.75	24888779 - 46440369
1b	PF2016	2.42	8	RW3@42.6	20.05	Rh12GR_52506_1218	42317122	37.69 - 42.55	41648024 - 42317122	35.67 - 42.55	40854291 - 42317122
	PF2017	2.38	8.31	RW3@42.6	12.94	Rh12GR_52506_1218	42317122	37.69 - 42.55	41648024 - 42317122	37.69 - 42.55	41648024 - 42317122
	PF2018	2.36	8.03	RW3@42.6	21.45	Rh12GR_52506_1218	42317122	37.69 - 42.55	41648024 - 42317122	37.69 - 42.55	41648024 - 42317122
	PM2016	2.51	5.88	RW3@42.6	12.76	Rh12GR_52506_1218	42317122	16.8 - 42.55	32557591 - 42317122	9.44 - 42.55	16767733 - 42317122
	PM2017	2.41	9.56	RW3@42.6	12.12	Rh12GR_52506_1218	42317122	37.69 - 42.55	41648024 - 42317122	35.67 - 42.55	40854291 - 42317122
	PM2018	2.5	11.5	RW3@42.6	37.40	Rh12GR_52506_1218	42317122	28.3 - 42.55	36807925 - 42317122	16.8 - 42.55	32557591 - 42317122
2	PM2016	2.31	2.89	OB4@30.6	11.64	Rh12GR_60129_183	52239028	20.53 - 48.59	46189407 - 56107784	5.77 - 48.59	33319795 - 56107784
	PM2017	2.49	3.15	OB4@30.6	13.18	Rh12GR_60129_183	52239028	11.81 - 48.59	36731337 - 56107784	4.43 - 48.59	30431277 - 56107784
	PM2018	2.51	3.3	OB4@30.6	10.35	Rh12GR_60129_183	52239028	11.81 - 48.59	36731337 - 56107784	7.78 - 48.59	34803638 - 56107784
3	PF2017	2.38	2.8	RW6@29.7	6.73	Rh12GR_56601_1304	31814891	8.11 - 42.49	4339433 - 44264630	0 - 48.52	1518964 - 48810479
	PF2018	2.36	2.81	RW6@11.5	6.67	Rh88_37299_454	5410244	6.74 - 44.11	7764439 - 62612495	1.34 - 54.05	1461254 - 64122872
	PM2016	2.51	4.16	RW6@29.7	8.45	Rh12GR_56601_1304	31814891	0 - 38.43	1518964 - 48896977	0 - 42.49	1518964 - 44264630
	PM2017	2.41	2.7	RW6@29.7	7.07	Rh12GR_56601_1304	31814891	15.59 - 45.19	8578645 - 45439915	8.11 - 49.9	4339433 - 41715319
	PM2018	2.5	2.58	RW6@29.7	5.28	Rh12GR_56601_1304	31814891	4.21 - 48.53	3340353 - 48180089	0 - 53.21	1518964 - 52689670
4	PF2016	2.42	3.08	RW1@34.2	6.52	RhK5_3678_875	59006755	12.78 - 44.11	20231658 - 62553371	6.74 - 54.05	7764439 - 64122872
	PF2018	2.36	3.04	RW1@34.2	6.99	RhK5_3678_875	59006755	6.74 - 44.11	7764439 - 62553371	1.34 - 54.05	3670420 - 64122872

<sup>a</sup>PT genome-wild LOD significance threshold was defined by a permutation test. <sup>b</sup>LG@positon chromosomal linkage group, using the separate map (OB and RW) numbering of (Hibrand-Saint Oyant et al., 2018) @ peak location in cM. <sup>c</sup>r(%) Percentage of explanation. <sup>d</sup>Closest molecular marker (MM) associated. <sup>e</sup>location in base pair (bp) on the *Rosa chinensis* Genome v1.0 (Hibrand-Saint Oyant et al., 2018). <sup>f</sup>centiMorgan position of QTL peak.





**Supplementary Figure 1**



**Supplementary Figure 2**



**Supplementary Table 1. Primer sequences of candidate genes for qPCR**

Primer name	sequence of primers
RcMYC1-1-F	5' CCACCCTCAATGATGTTCTC 3'
RcMYC1-1-R	5' TTCTGGCGTCTCAACACTTAC 3'
RcTT8-1-F	5' AGAGAGCGATGGATTGTTGG 3'
RcTT8-1-R	5' GCCCTCTTCACTTCTGTAATGG 3'
RcGIS2-1-F	5' CTGGTGACTCCGTTGTTCG 3'
RcGIS2-1-R	5' TCCCTAAGATGGATGGATTGA 3'
RcGIS3-1-F	5' GGCCATCGTTGAGTAGGTTC 3'
RcGIS3-1-R	5' GGAGTCAGAGGCTGAGTTGC 3'
RcTRY-1-F	5' GGAAAGCAGAAGAAATAGAGAGG 3'
RcTRY-1-R	5' CTACTACTGACAAGGAAAACCAATG 3'
RcTTG1-1-F	5' TCCAATGTCAATGTACTCGGC 3'
RcTTG1-1-R	5' CCTCCTCAAACCTTCAACAGC 3'
RcTTG2-1-F	5' CCTCAAACCCAGGAGCATC 3'
RcTTG2-1-R	5' CAACAGCTTGATCCCTGAGAG 3'
RcCPC-F	5' GACATTGTGAGGTGTTTGCTGAG 3'
RcCPC-R	5' AATCCGCTGAAAGTTCGACG 3'
RcMYB61-F	5' GGATCTTCAGAGACTCGCTGTAGC 3'
RcMYB61-R	5' CAAGCCCTCCTCTCACATTCAT 3'
RcZFP5-F	5' CAGGAGAAAGCAGACCAGTGAT 3'
RcZFP5-R	5' GGCAAGCCAATCCCTAACTG 3'

**Supplementary Table 2. Summary of QTLs for NGP with two-part QTL model in OW progeny**

Trait	Phenotyping	PT <sup>a</sup>	QTL Characteristics			
			LG@positon <sup>b</sup>	MM <sup>c</sup>	bd <sup>d</sup>	r(%) <sup>e</sup>
Binary(p)	PF2016	2.57	OB3@44.4	Rw35C24	40,215,502	15.93
	PF2017	2.53	OB3@44.4	Rw35C24	40,215,502	15.18
	PF2018	2.6	OB3@44.4	Rw35C24	40,215,502	16.12
	PM2016	2.47	OB3@44.4	Rw35C24	40,215,502	14.76
	PM2017	2.58	OB3@44.4	Rw35C24	40,215,502	13.38
	PM2018	2.51	OB3@44.4	Rw35C24	40,215,502	16.72
	PF2016	2.67	RW3@42.6	Rh12GR_52506_1218	42,317,122	29.31
	PF2017	2.59	RW3@42.6	Rh12GR_52506_1218	42,317,122	30.33
	PF2018	2.57	RW3@42.6	Rh12GR_52506_1218	42,317,122	28.72
	PM2016	2.54	RW3@42.6	Rh12GR_52506_1218	42,317,122	20.69
	PM2017	2.56	RW3@42.6	Rh12GR_52506_1218	42,317,122	26.84
	PM2018	2.59	RW3@42.6	Rh12GR_52506_1218	42,317,122	33.21
	PF2016	2.67	RW2@16.2	CTG356	1,674,220	1.80
	PM2016	2.47	RW6@22.3	RhMCRND_12897_444	17,698,816	2.70
	PF2016	2.42	OB4@30.6	Rh12GR_60129_183	52,239,028	9.02
	PM2016	2.36	OB4@30.6	Rh12GR_60129_183	52,239,028	9.26
	PM2017	1.92	OB4@30.6	Rh12GR_60129_183	52,239,028	9.88
	PM2018	2.8	OB1@67.7	Rh12GR_62822_144	7388536 and 7,633,108	6.66
Quantitative(μ)	PF2016	2.39	RW3@42.6	Rh12GR_52506_1218	42,317,122	20.98
	PM2016	2.26	RW3@28.3	Rh12GR_78941_279	36,727,828	14.23
	PM2017	1.88	RW3@32.3	Rh88_36897_190	38,554,327	12.61
	PM2018	2.52	RW3@42.6	Rh12GR_52506_1218	42,317,122	38.64
	PF2018	2.57	RW1@24.1	Rh88_6034_211	45,638,457	7.80

<sup>a</sup>PT genome-wide LOD significance threshold was defined by a permutation test. <sup>b</sup>LG@positon chromosomal linkage group, using the separate map (OB and RW) numbering of (Hibrand-Saint Oyant et al., 2018) @ peak location in cM. <sup>c</sup>Closest molecular marker (MM) associated. <sup>d</sup>location in base pair (bp) on the *Rosa chinensis* Genome v1.0 (Hibrand-Saint Oyant et al., 2018). <sup>e</sup>r(%) Percentage of explanation.

**Supplementary Table 3 Summary the rose homologies genes know in *A. thaliana* to be involved in trichome initiation**

Family	AT genes	Function description	Mutant vs WT	Rose gene name	Rose geneID	Genome location
R2R3MYB	AT3G27920/GL1	Interacts with JAZ and DELLA proteins to regulate trichome initiation	No trichome	RcGL1	RC7G0156100	Chr07:11958961..11961286 (2.33 Kb)
	AT5G52600/MYB82	MYB82 and GL1 can form homodimers and heterodimers at R2R3-MYB domains. At least one of the two introns in MYB82 is essential to the protein's trichome developmental function		RcMYB82	RC2G0033100	Chr02:2470719..2472719 (2 Kb)
	AT1G09540/MYB61	Affects trichome initiation, root development and stomatal aperture	Fewer trichome	RcMYB61	RC3G0322900	Chr03:39896892..39899077(2.18kb)
R3MYB	AT2G46410/CPC	Positive regulator of hair-cell differentiation. Preferentially transcribed in hairless cells.	Increase density	RcCPC	Chr1g0359121	Chr01:47708266..47710558bp(2.32kb)
	AT5G53200/TRY	Involved in trichome branching	cluster phenotype	RcTRY	RC1G0560100	Chr01:62070383..62072848(2.47 Kb)
bHLH	AT5G41315/GL3	Encodes a basic helix loop helix domain protein that interacts with GL1 in trichome development. GL3 interacts with JAZ and DELLA proteins to regulate trichome initiation.	Fewer trichome	RcGL3	RC7G0190300	Chr07:15536877..15543259 (6.38 Kb)
	AT4G09820/TT8	TT8 is a regulation factor that acts in a concerted action with TT1, PAP1 and TTG1 on the regulation of flavonoid pathways, Also important for marginal trichome development.	Fewer trichome	RcTT8	RC6G0407800	Chr06:52002793..52009528 (6.74 Kb)
	AT4G00480/MYC1	MYC-related protein with a basic helix-loop-helix motif at the C-terminus and a region similar to the maize B/R family at the N-terminus	Fewer trichome	RcMYC1	RC1G0342400	Chr01:44468298..44473643 (5.35 Kb)
WD40	AT5G24520/TTG1	Involved in trichome and root hair development. Controls epidermal cell fate specification.	No trichome	RcTTG1	RC1G0586100	Chr01:63982095..63985616 (3.52 Kb)
WRKY	AT2G37260 /TTG2	Trichome development	Trichome clusters and a reduced trichome number	RcTTG2	RC3G0244800	Chr03:33397852..33403551 (5.7 Kb)
C2H2	AT1G10480/ZFP5	Acts downstream of ZFP6 in regulating trichome development by integrating GA and cytokinin signaling.		RcZFP5	RC4G0476500	Chr04:57125905..57127513 (1.61 Kb)
	AT1G68360/GIS3	GIS3 is involved in trichome initiation and development downstream of GA and cytokinin signaling.		RcGIS3	RC4G0390900	Chr04:50315805..50317009 (1.21 Kb)
	AT1G80730/ZFP1	Expressed at high levels in the shoot apex, including the apical meristem, developing leaves and the developing vascular system		RcZFP1-like1	RC2G0415300	Chr02:47908413..47909551 (1.14 Kb)
				RcZFP1-like2	RC6G0454700	Chr06:55856328..55858302 (1.98 Kb)
	AT5G06650/GIS2	Regulates trichome formation on inflorescence stems; is also influenced by cytokinins		RcGIS2	RC3G0150000	Chr03:23331984..23333173 (1.19 Kb)
HD-ZIP IV	AT1G79840/GL2	A homeodomain protein affects epidermal cell identity including trichomes, root hairs and seed coat		RcGL2	RC2G0467100	Chr02:54366345..54368366 (2.02 Kb)
					RC2G0467200	Chr02:54367536..54371324 (3.79 Kb)
					Chr2g0138951	Che02:54366345..54371324(5.81 Kb)

**Supplementary Table 4 Prickle number on four internodes of two types of stems for three years in OW progeny**

Individuals	PF2016	PF2017	PF2018	PM2016	PM2017	PM2018
Ow9001	0.67	5	2.67	10	12.67	10.33
Ow9003	0	0	0	14	12.33	8.33
Ow9004	2	3	0.33	3	3	0
Ow9005	10.67	12	11.67	10.67	12.33	11
Ow9006	3.67	4	9	3.67	4	0
Ow9007	3.67	4.67	8.33	10	4.67	5.67
Ow9008	6	0.67	0	6	2.67	1.33
Ow9009	7	4.33	2	7	5.33	12.33
Ow9010	11.67	11	7.67	11.67	15.67	12.67
Ow9011	11	11.67	9	11	11.67	11.67
Ow9012	11.67	14.67	11.67	15	17	14.33
Ow9013	1	2.67	4	2.67	2.67	4
Ow9014	2.33	10	0.67	9.67	10	2
Ow9016	NA	NA	NA	8.33	NA	NA
Ow9017	15.67	17	14.33	15.67	18.33	14.67
Ow9018	9.67	8.67	11.33	9.67	8.67	10
Ow9019	0	0	0	0	0	0
Ow9021	13.67	15.33	14.67	13.67	15.33	14.33
Ow9022	9.67	10	7.67	11.33	9.67	9.33
Ow9023	15.33	15.67	13.67	15.33	15.67	14.33
Ow9024	16	13	11.33	16	16.67	16.33
Ow9025	14	13	11.67	14	13	13.67
Ow9027	13	8.67	8.33	13	8.67	9
Ow9029	10	10	7.67	10	10	8.33
Ow9030	10.67	10.67	11.67	12	11	11.33
Ow9031	12.33	12.33	8.33	12.33	12.33	15.33
Ow9032	9.33	6.67	3.33	14.33	2	0.33
Ow9033	12.33	11	9	12.33	12	13.33
Ow9034	15.67	17.33	13.33	15.67	17.33	15
Ow9035	14	15	16.67	14	15	5
Ow9036	0	0	0	0	0	0
Ow9037	0	0.67	2	0.33	0.67	1
Ow9038	0	0	0	7.67	2.33	5.33
Ow9039	10.33	13	10.33	13.67	12	14.33
Ow9040	11.67	11.67	9	11.67	12	10.33
Ow9041	5.67	6.67	8.67	5.67	6.67	10.33
Ow9042	11.67	9.67	13	11.67	12.67	13.67
Ow9044	0.67	1	0.67	3.33	1	0
Ow9045	3.33	4.33	4.33	3.33	2.67	3.67
Ow9046	0	0.33	4	12.67	0.33	0.33
Ow9047	4.33	2	6	4.33	2	0
Ow9049	1	0	4	1	0	0
Ow9050	14	15.33	16	14	15.33	13.33
Ow9051	0.67	0.33	0	0.67	0.33	0.33
Ow9052	13.67	14.33	12.33	16.33	14.33	12.33
Ow9054	0	0	0	0	0	0
Ow9055	6.67	6.67	9.33	6.67	11	11.67

Ow9056	NA	0	0	0	0	0
Ow9057	0	0	0	0	0	0
Ow9058	NA	0	0	0	0	0
Ow9059	0.33	1.33	0.33	0.33	1.33	0.67
Ow9060	1	1.33	2.67	1	1.33	1
Ow9061	12.67	12	9.33	11.33	12	12.33
Ow9062	12.67	9.67	7.67	14.67	14.33	14.67
Ow9065	2	1.67	0	3.67	8.67	4
Ow9066	2.33	6.33	3.67	10.67	10	11
Ow9067	0	0	0	0	0	0
Ow9068	0	0	0	0	0	0
Ow9069	14.33	14.67	11	14.33	14.67	13
Ow9071	14	21.33	12.67	18.67	16	13.67
Ow9072	16.67	16.67	13	16.67	16.67	12.33
Ow9074	11.67	11	10.33	11.67	11	5.67
Ow9075	11.67	14	9.33	11.67	14	12.67
Ow9076	2.67	3	1.67	11.67	3	0
Ow9077	10.67	9.67	10.33	10.67	15	14.33
Ow9078	0.67	0	0	0.67	0	0
Ow9079	11.67	8.67	7.67	11.67	12	12
Ow9080	12.67	10.33	9.67	13.33	16.33	12.33
Ow9081	13	13	12.33	13	15	15.33
Ow9082	9.33	12	11.33	9.33	12	11.33
Ow9083	12	9	9	12	9	12
Ow9084	14.33	14	13.67	15.67	20.33	17
Ow9085	12	3	10	12	12	13
Ow9087	14.33	15	12.67	14.33	15.33	14.67
Ow9088	10.33	11.33	10.33	12.33	11.33	11
Ow9089	13.33	13.67	13	13.33	15	15.33
Ow9091	0.67	1	0.67	0.67	1	0
Ow9092	8	7.33	8.33	15.67	12	6
Ow9095	11	11.33	7.33	11	11.33	12.33
Ow9096	5.67	10.67	9.33	9.67	10.67	11
Ow9098	2.67	10.67	9.33	9.33	11	11.33
Ow9099	13.33	12	14.67	13.33	12.67	9.33
Ow9100	6.67	8	8.33	6.67	8	9.33
Ow9101	15	16	11.33	15	15	17.33
Ow9103	15	8.67	11	15	15	14.33
Ow9104	10.67	12.33	9	13	11.67	13
Ow9105	12.67	12	8	12.67	12.33	12
Ow9106	43	45.67	38	48.67	48	30
Ow9107	38	52	35	32.33	42.33	29
Ow9109	12	10.67	9.67	12	10.67	11.33
Ow9111	6	2.67	0.33	16.33	2	10.33
Ow9113	15.67	14.33	13.33	15.67	18.33	13.33
Ow9115	6.67	0.33	0.33	6.67	6	1.33
Ow9116	12	12.67	12	12	12.67	11.33
Ow9117	13.33	14	15	15	16	14.33
Ow9119	0	0	0	0	0	0
Ow9120	8	10	9.33	8	10	7
Ow9121	4.67	5.33	5.67	11.67	10.33	9.67

Ow9122	9	9.67	10.67	9	9.67	7.33
Ow9123	11.67	7.67	7.67	10	9	9
Ow9124	5	10	9.67	12.67	12.67	12.67
Ow9125	7.67	9	7	11.33	11.67	9.33
Ow9126	9.67	15	10	24	20.33	12.33
Ow9127	13.33	11.67	8.67	13.33	11.33	11
Ow9128	0	1.33	0	0	1.33	1.33
Ow9129	5	10.67	11.33	12	11	11.33
Ow9132	0	0	0	0	0	0
Ow9133	0.67	1.67	0	0.67	1.67	0
Ow9134	18	13.67	16.67	18	13.67	18.67
Ow9137	5	7.67	3.67	8.33	11	8
Ow9138	10.67	10	8	15	15.67	12.33
Ow9139	18.67	20	20	17.33	17.33	15
Ow9140	6.67	9	9	6.67	11.67	10.67
Ow9142	10.67	10.33	9.67	10.67	10.67	12.67
Ow9143	16.67	12	9.33	13	12.33	9.33
Ow9144	21.33	15	16	16	14.33	14.67
Ow9147	16.33	18	13.67	16.33	18	11.33
Ow9148	NA	16	16	NA	16	8
Ow9149	0	0	0	0	0	0
Ow9150	0	0	0	0	0	0
Ow9151	NA	12.33	12	NA	12.33	13.33
Ow9152	13.33	13.33	16.33	13.33	15	20
Ow9153	0	2.33	2.33	3.67	2.33	3
Ow9154	16.33	15.33	15.33	16.33	15	12.33
Ow9155	8	9	9	11.67	11.67	10.33
Ow9156	8.33	8	7.67	11.67	11.67	10.67
Ow9158	NA	9	3	NA	8.67	4
Ow9159	9.67	10	10.67	11	12.33	11.33
Ow9160	17	15.33	10	12	12.33	14.33
Ow9161	10.33	9.67	10	10.33	12	7.33
Ow9163	0.67	2.33	0	0.67	2.33	0.67
Ow9166	0	0	0	2	0	0
Ow9167	11	9.67	10	11	9.67	10
Ow9168	6.33	9	7	6.33	9	6
Ow9169	10.67	10.67	11	10.67	10.67	11.33
Ow9171	0	0.67	0	0	0.67	0
Ow9172	13.33	16.33	17	13.33	16.33	15.33
Ow9173	NA	16.67	16.67	NA	16.67	16.67
Ow9174	NA	8	8	13.33	8	5.33
Ow9175	11.67	9	8.33	13.33	14	12.33
Ow9178	0	0	0	0	0	0
Ow9179	12.67	13	12.33	12.67	12.67	16.33
Ow9180	11	10.33	10.67	11	11.33	12.33
Ow9181	0	0	0	0	0	0
Ow9182	7.67	NA	7.67	9.67	NA	3.67
Ow9185	12.67	11.33	11.67	12.67	11.33	11.67
Ow9186	0	NA	2.67	4.67	NA	2
Ow9190	11.67	16.33	10.67	11.67	13	13
Ow9191	2.67	7.33	7.67	9.67	9	8.67

Ow9192	8.33	10.33	9	12.67	11.33	11.33
Ow9197	19	19	18.33	19	16.33	17

---